EC DG Research

Contract No EVK2-CT-2002-00179

Land Degradation Assessment in Mediterranean Europe

Contribution to the GMES Full Details Report 2003

Reporting period: 01/12/2002 – 31/08/2003

Consejo Superior de Investigaciones Científicas
Estacion Experimental de Zonas Aridas
EEZA CSIC

Universidade Nova de Lisboa
Faculdade de Ciências Sociais e Humanas

Universität Trier
Remote Sensing Department

RIKS
research institute for knowledge systems

EUROPEAN COMMISSION
DIRECTORATE GENERAL JRC
JOINT RESEARCH CENTRE
Institute for Environment and Sustainability
Soil and Waste Unit

Contents

WP1 - Project management

The project management comprises a variety of activities related to the administrative and organisational framework of the project. It is running in parallel to the project and naturally covers the full project period

The organisation, administration and management of the project as well as technical support and the maintenance of data storage facilities, furthermore the dissemination of the project's philosophy and results are tasks which are covering the full project period. As main deliverables the project data server and the project website have been implemented. Besides, the project management focuses on data sets acquisition during the first reporting period (see also fig. LADAMER data flow and availability).

1.1 Milestones and deliverables obtained

During the first nine month of the project LADAMER obtained main milestones:

- Project Kick-off meeting held at Ispra, Italy (Oct'02).
- Agreement on LADAMER data flow and necessary data sets for assessment and modelling land degradation (Oct'02) (see fig. LADAMER data flow and availibilty).
- Second project meeting held at Ericeira, Portugal (May'03).
- First version of the website is on-line (May'03).
- The team has reached an agreement on reference coordinate system and resampling strategy for gridded data sets (May'03).
- Almost every planned data sets have been made available to the LADAMER project team (May'03) (see fig. LADAMER data flow and availability).
- 1st Management report (July'2003)

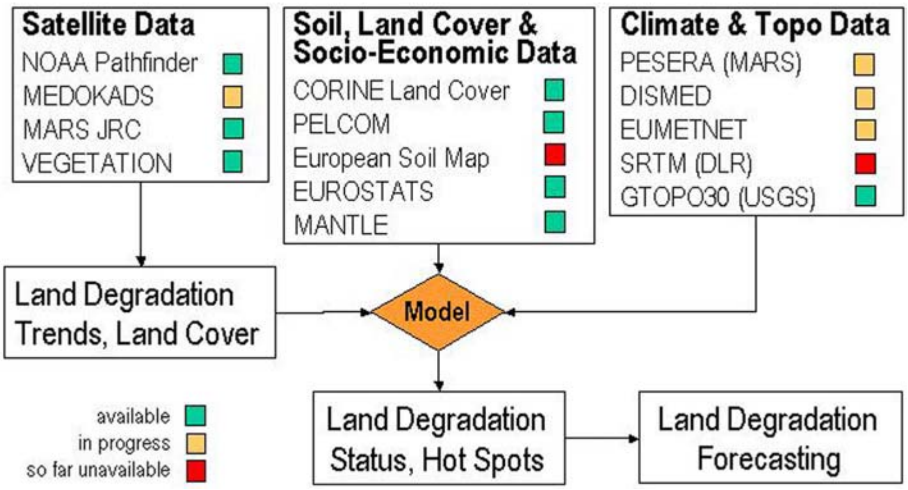

Figure 1: LADAMER data flow and availability

1.2 Deviations from the work plan or time schedule and their impact to the project

Due to the tight schedule of the first phase of LADAMER according to the restrictions of GMES phase I the Kick-off meeting of the project was carried out almost two months ahead of the official project start. This advance won almost two months in data acquisition and made the later change of the date of the fourth GMES forum compensable.

The acquisition of satellite and ancillary data has been more time-consuming than expected, mainly due to problems with administrations in charge of most of ancillary data such as digital elevation models, soil data base, statistical data etc. The European Soil Data Base is still not available to the LADAMER project due to national restrictions in distributing this essential data set. Data sets which have already been paid by the European tax payers (statistical data) had to be obtained from institutions (EUROSTATS) for high costs burden on the LADAMER project budget.

1.3 Co-ordination of the information between partners and communication activities

The co-ordination of the information between partners and communication activities is one of the major tasks of the LADAMER project management. To fulfill this issue representatives of UTRIER presented the conceptional framework and preliminary results of the LADAMER project at several meetings:

- Project Kick-off meeting hosted by Joint Research Centre / Soil and Waste Unit (partner 4) in Ispra / Italy, October 5th-and 6th 2002.
- Presentation of preliminary outputs of LADAMER project at the second GMES Forum held at Noordwijk, January 14th - 16th, 2003
- Presentation of LADAMER project at the GMES project co-ordinators meeting held at Brussels, March 27th, 2003.
- Presentation of preliminary outputs of LADAMER project at the third GMES Forum held at Athens, June 5th - 6th, 2003
- 2nd project meeting hosted by Departamento de Geografia e Planeamento Regional / Faculdade de Ciências Sociais e Humanas of the Universidade Nova de Lisboa (partner 5) in Ericeira / Portugal, May 5th-and 6th 2002.
- Presentation of LADAMER project at the BIOPRESS project meeting held at Dresden, August 25th-27th 2003.

Among other data sets NOAA Pathfinder data sets have been made available for time series and trend analysis as well as NOAA Mars data. Furthermore the project received access to the NOAA MEDOKADS data base. So far the full time series for the Iberian Peninsula was made available. Assess to the CORINE land cover from the EAA have been achieved. The EU light emissions data base compiled in the context of the European research project MANTLE has been made available to LADAMER for further use in modelling land use change and to assess land degradation. Assess to SPOT VEGETATION data sets have been organised and continuous up-date of newly available scenes has been arranged. The MEDOKADS NOAA AVHRR 1km data base have been made partially available to the LADAMER project.

Co-operation with the BIOPRESS team will make backdated CORINE land cover data available for the LADAMER project. BIOPRESS offered as far as acceptable for their project to work primary on BIOPRESS test sites which are of interest for the LADAMER project. The LADAMER project management was invited to present LADAMER at the BIOPRESS meeting held at Dresden (26th – 28th August).

An internal section at the website has been established on which LADAMER partners can extract project related documents (e.g. working documents, presentations etc.).

Assess to the project server via FTP has been enabled which allows the LADAMER project partners down-load and up-load of data sets and documents. A regularly updated meta-database is almost completed.

UTRIER has supported, from a logistical point of view, EC-JRC-SWU to make NOAA-AVHRR time series data sets from MARS project available to the LADAMER partners by sending a staff member for five weeks to the JRC (17th March – 17th April 2003). Additional, technical support have been given to RIKS for data set re-projection to reference coordinate system.

WP2 - Geoinformatics and remote sensing data analysis

2.1 Integrated geo-database

The first deliverable of WP2 is the generation of an integrated geo-database. Therefore relevant sources of data necessary for the project were ordered and collected. The data are hosted on a server which guarantees free access for the project partners. Needed data can be downloaded by the partners via FTP.

Among other data sets the 8 km NOAA AVHRR Pathfinder data set (1981-2002) has been made available for time series and trend analysis as well as the NOAA AVHRR Mars time series (1989-2002). Furthermore the project received access to the 1 km NOAA AVHRR MEDOKADS data base. So far the full time series (1989-2002) for the Iberian Peninsula was made available. Also access to the CORINE land cover from the EAA has been achieved. The EU light emissions data base compiled in the context of the European research project MANTLE has been made available to LADAMER for further use in modelling land use change and assessing land degradation. SPOT VEGETATION data sets (S1-product) can be downloaded freely via Internet, and continuous up-date of newly available scenes has been arranged. At the moment only an older version of the European Soil Map (Version 2, 09/2000) is free available, because still difficulties exist concerning the distribution of the new updated data set.

Furthermore it is of major interest to generate metadata at an appropriate level to guarantee data applicability of the hosted data sets, to keep track of error propagation and to enable information dissemination to end-users in an adequate way. The partners decided to follow the Geographic Data Committee's (FGDC) Content Standard for Digital Geospatial Metadata, which is implemented in the software-package ArcGIS. It is similar to the ISO standard 19115 (Geographic Information – Metadata). Thus, it is guaranteed, that all hosted datasets and new produced information layers receive are well documented.

2.2 Vegetation trend analysis and hot spot detection

The analysis of regional degradation dynamics and hot spots asks for longer (i.e. minimum 10 years) time series of small-scale satellite images. In this context it seemed to be advisable to use NOAA AVHRR datasets, because this sensor is the only existing source of long-term high temporal resolution land surface data, like for example the 8 km NOAA AVHRR Pathfinder dataset (1981-2002) and the 1 km NOAA AVHRR MEDOKADS dataset (1989-2002).

Information layers derived from the implemented time series analysis procedures are maps of vegetation trends and their significance. Out of these results hot spots of land degradation are detected. A further interpretation of these products requests thematic layers like for example the Corine Land Cover Classification.

The provided maps can support decision makers on EU and national level to receive an overview which regions in the Mediterranean are concerned by changes in vegetation cover, positive as well as negative. Especially regarding negative trends, investigations have to be carried out which developments or incidents caused the detected vegetation changes, which are responsible for the identified hot spots. If these changes are anthropogenic and lead to land degradation, considerations have to be made in which regions new policies have to be implemented to avoid a proceeding of land degradation.

The methodological procedures were developed based on the 8 km NOAA AVHRR Pathfinder dataset. Afterwards these procedures were applied on the NOAA AVHRR MEDOKADS time series.

2.2.1 Pre-processing

First of all missing values and outliers were removed from the data set and the gaps were filled using linear interpolation.

The precision of the AVHRR visible channels degenerates rapidly in areas with low illumination. For that reason, all data with a solar zenith angle greater than 80 degrees are excluded from the processing procedure. This is most pronounced at the summer and winter solstice (DeFries et al., 1998; NASA, 2002c).

Outliers are measurements that are extremely large or small relative to the rest of the data and, therefore, are suspected of misrepresenting the population from which they were collected. Outliers may result from measurement system errors such as instrument breakdown or temporary system failure. However, outliers may also represent true extreme values and indicate higher variability in the data set than was expected. Not removing true outliers and removing false outliers both lead to a distortion of analysis results (EPA, 2000; Hartung, 1995).

To reduce the effects of noisy data in the Pathfinder time series, spikes in the temporal NDVI profiles were identified by locating those pixels that are more than 3 standard deviations away from the mean value of the remaining data.

Unfortunately, long time series from different satellites may be affected by a number of factors that are independent from surface parameters, including different instrument calibration, sensor degradation, and changes in viewing-geometry. Some of these parameters may cause sharp discontinuities, while other changes, such as the shift in equatorial crossing time, causes gradual biases in the data. It is important to detect and, if necessary, remove these inhomogeneities. For that, homogeneity tests were applied. Thus an orbital drift of NOAA AVHRR since 1999 could be detected in the NOAA AVHRR Pathfinder data. This result led to the decision to perform the time series analysis only till 1999.

Some trend analysis tools like the linear regression require elimination of time series cycles. So before performing the trend analysis for these approaches, the annual vegetation cycle was eliminated.

2.2.2 Trend analysis and hot spot detection

After the preparatory data analysis of the time series, trend analysis was performed on this data. Different approaches to detect trends in the data were implemented, as there are i.e. linear regression, Mann-Kendall-test, Seasonal Kendall and Modified Seasonal Kendall test.

In an additional step, the influence of the spatial resolution of the two datasets on the results of time series analysis was examined. Therefore the time series analysis for the Pathfinder dataset which covers a longer time period than the MEDOKADS dataset was also performed for the time period from 1989-1998.

The analysis of the time series showed positive trends for the deserts in North-Africa. This “greening of the deserts” is a problem because this area is mainly free of vegetation and should not show any trend in the NDVI values. Therefore an attempt was performed to eliminate these underlying trends from both time series. This procedure can be only carried out, if the trend underlies the whole examined scene. The Pathfinder data mainly showed no significant trend in the desert area after a linear trend correction. The MEDOKADS data could not be corrected, because the trend seems not to be linear. Further investigations have to be undertaken to describe and eliminate this trend component. Nevertheless both datasets showed the same areas concerned by negative trends with a high significance.

The task of deriving hot spots from the vegetation trend classes proved to be difficult due to the ill-defined term “hot spot”. Hot spots can simplified be described as areas which show a highly significant trend. But this trend can be caused by different developments and incidents. Thus hot spots of negative vegetation trends can be a consequence of fire incidents, changes of land cover or climatic parameters. In the case of land cover change a negative trend in vegetation cover can cause simply a leap from higher NDVI values to lower ones. Whereas in the other case a steady decline of the vegetation cover can be reason for a hot spot and thus a hint on a wrong land use. Currently, different approaches are implemented to detect hot-spot areas.

Regarding the interpretation of the trend classes and the hot-spots, it is important to take into consideration thematic layers like maps of land cover. Unfortunately at the moment only Corine Land Cover 1990 is available, because the update Corine Land Cover 2000 is still not completed. But for the interpretation if a land cover change causes land degradation it is necessary to possess at least land cover maps of two different time steps. Thus land cover changes can be detected, followed by an examination, if these land cover changes cause negative trends of the vegetation cover, which can lead to land degradation. Therefore a multi temporal land cover classification was started on the 1 km NOAA AVHRR MEDOKADS data. In this way two comparable land cover maps will be created of two different dates (1990 and 1998). This concept is described later on.

2.2.3 Results

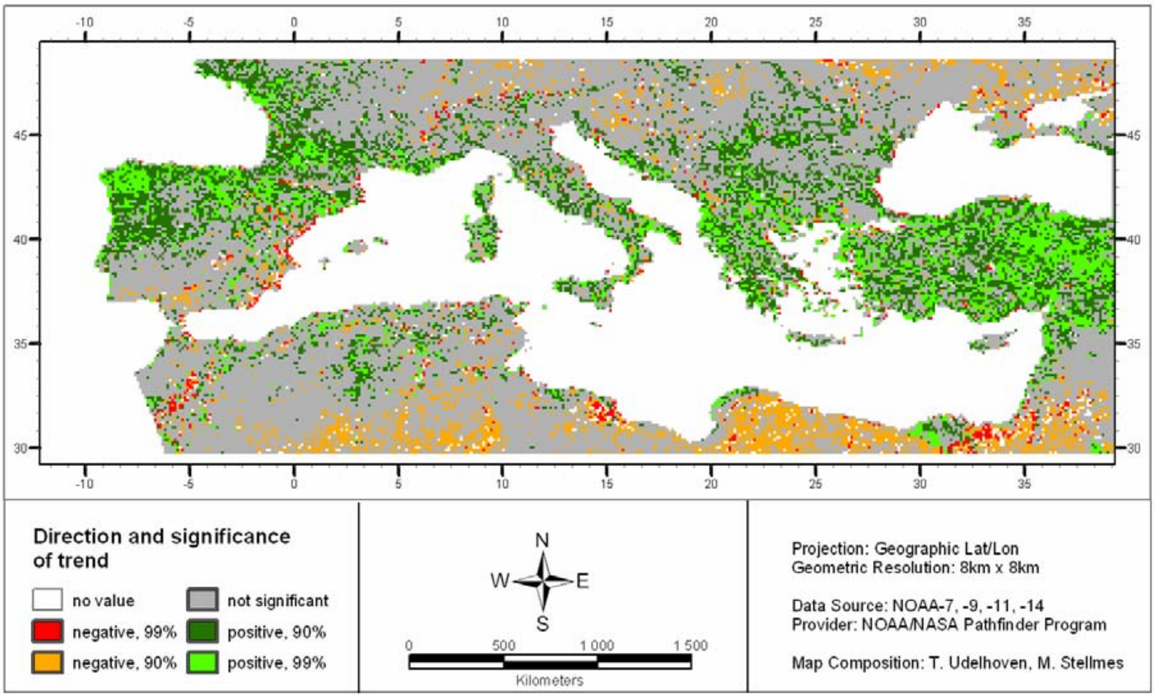

Figure 1: Direction and significance (T-Test) for the linear regression performed on the annual means of the NOAA AVHRR Pathfinder time series for the Mediterranean area covering the time period 1989-1999.

Figures 1 and 2 show the results of the trend analysis for the Pathfinder and the MEDOKADS time series. It was performed using linear regression on the annual NDVI mean values covering a time period from 1989 to 1999. The significance of trends was examined implementing a t-Test. As the Pathfinder data set is already trend adjusted, the MEDOKADS dataset still shows the "greening of the deserts"-effect. Nevertheless both datasets reveal the same areas of negative and positive trends on the Iberian Peninsula, i.e. Valencia.

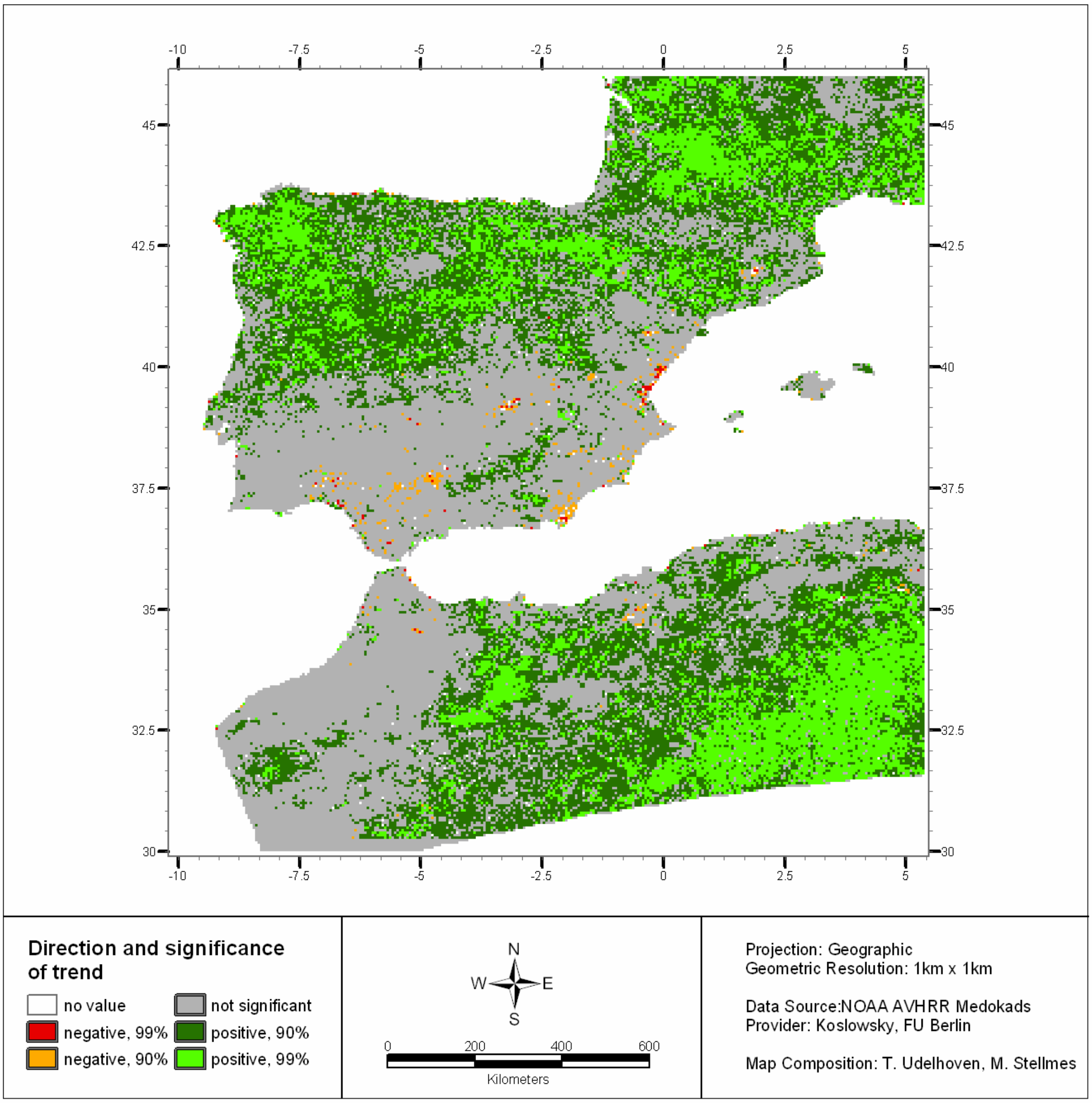

Figure 2: Direction and significance (T-Test) for the linear regression performed on the annual means of the NOAA AVHRR MEDOKADS time series for the Iberian Peninsula covering the time period 1989-1999.

Subsequently a case study of the Valencia region is presented. Figure 3 shows a subset of the results of the Pathfinder and MEDOKADS time series analysis for the Valencia region. When comparing both results, it has to be kept in mind, that for the MEDOKADS data still a positive trend is underlying, which falsificates the result. Removing the trend would reduce the positive trends and amplify negative.

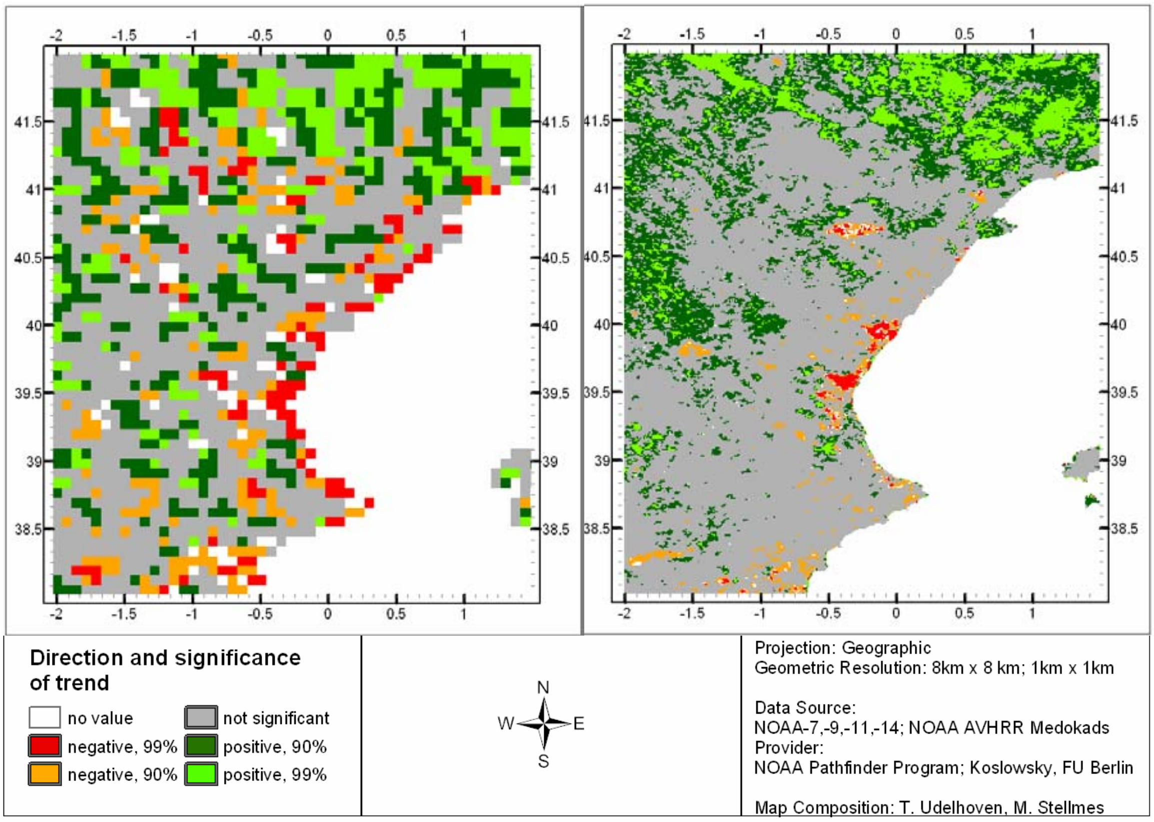

Figure 3: Direction and significance (T-Test) for the linear regression performed on the annual means of the NOAA AVHRR Pathfinder (left) MEDOKADS (right) time series covering the time period 1989-1999 for the Valencia region.

As visible in figure 3, the coastal area around of the city of Valencia is characterized by an accumulation of pixels displaying significant negative trends, which might be triggered by two different processes: urbanization and intensification of agriculture.

The Valencia region stretches out along the Spanish Mediterranean coast, between Catalonia in the north and Murcia in the south. Its landscape is diverse, with mountains in the west and littoral plains on the Mediterranean side, whereas the southern part is characterized by hills (European Commission, 2002; Walker, 1999).

Spain's coastal area around the city of Valencia has been suffering from strong urban development over the last two decades (Calzada, pers. comm.). The concentration of population and economic activities on coastal spaces, combined with tourist urbanization, severely impacts local ecosystems. NDVI values are influenced by the loss of vegetation cover due to large area sealing of soil caused by the construction of buildings and associated infrastructure.

The region's main agricultural products are oranges and other citrus fruits, because local climate conditions around Valencia are ideal for intensive citriculture. Winters are mild and rainy and the all year warmth has only minimal diurnal temperature fluctuations. Consequently, about 80 % of Spain's annual production of oranges is located in the Valencia region. Irrigation systems and additional nutrient supply are wide spread in order to increase crop yield (Walker, 1999).

Approximately 40 % of the total farmland is under irrigation. Water supply is generally suffcient due to the existence of an underground aquifer. Nevertheless, irrigation may trigger severe environmental damages, such as water pollution, groundwater exhaustion, salinization and surface erosion, the latter being a serious problem in the Valencia region (European Commission, 2002; Kok et al., 1995). For the extensive cultivation of citrus fruits the natural vegetation cover is removed and the unprotected top soil is easily carried away by precipitation. Compared with the natural vegetation, the spatial fraction of photosynthetic active vegetation is noticeably lower, and consequently NDVI values as well (Erbrecht, 2003).

2.3 Vegetation density assessment

An essential component of the land degradation status assessment product is the availability of a homogeneous information layer on vegetation density, which allows a quantitative analysis of the vegetation cover, in contrary to the NDVI, which is a relative measure for the vegetation density.

2.3.1 Spectral Unmixing

To solve this task a spectral unmixing strategy was implemented which uses the vegetation index NDVI and the land surface temperature. This method is performed on the 1 km NOAA AVHRR MEDOKADS dataset.

The implemented spectral unmixing approach acts on the assumption, that vegetation cover should predominantly control the position of an AVHRR land surface pixel within the feature space spanned up by NDVI and surface temperature (European Commission, 1998). Thus, linear approximations to explain NDVI as well as surface temperature of mixed AVHRR pixels (vegetation and non-vegetation) in relation to vegetation have been given.

According to Price (1993) the NDVI of mixed pixel can be expressed as:

$$NDVIp = f(NDVIv) + (1 - f)NDVIn$$

where f = fraction of vegetation
v = vegetation
n = non-vegetation

The surface temperature accordingly was obtained by Caselles and Sobrino (1989):

$$Tp = f \cdot Tv + (1 - f)Tn$$

where T = temperature
f = fraction of vegetation
v = vegetation
n = non-vegetated

Thus a 3 endmember mixing model with the endmembers “fully vegetated” (100% vegetation coverage), “non-vegetated” (absence of vegetation) and “water” (i.e. temperature variability) was implemented. These three endmembers are spectrally distinct enough to define a robust model to explain most land pixels under the aspect of vegetation cover estimates. Thereby the “water” endmember works similar to the shadow endmember in the common unmixing approach. It compensates effects like local gradients related to altitude and exposition, temperature variations due to soil moisture, furthermore to variable evaporation and evapotranspiration respectively.

The definition of the endmembers is the crucial point of the spectral unmixing approach and thus determines the quality of the unmixing. The implementation of the spectral unmixing model followed the description given in the DeMon-II final report (European Commission, 1998).

2.3.2 Preliminary results

Figure 4 shows the derived vegetation density for the Iberian Peninsula in April and September 1990.

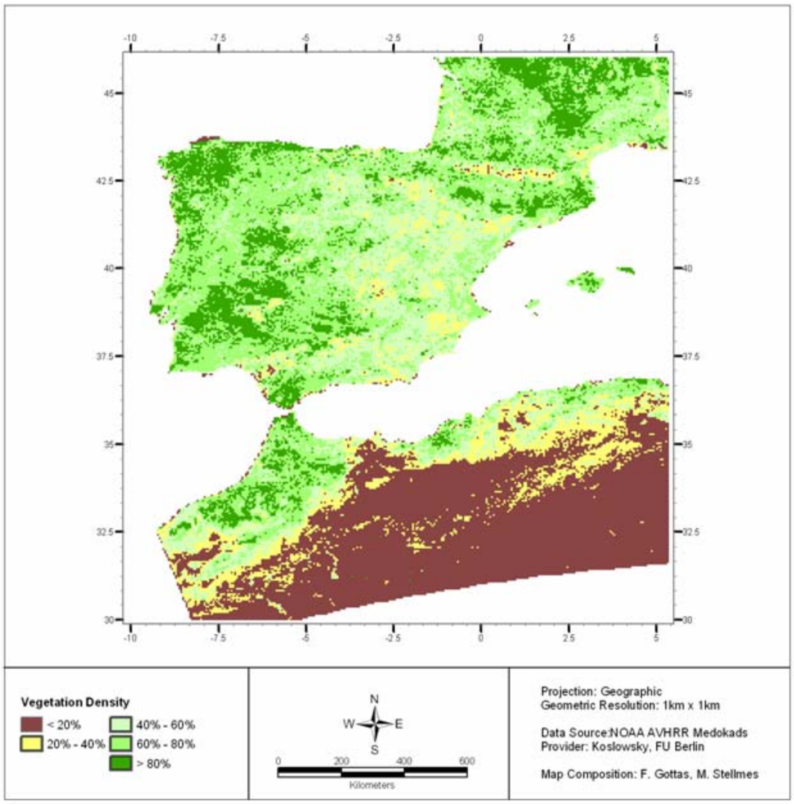

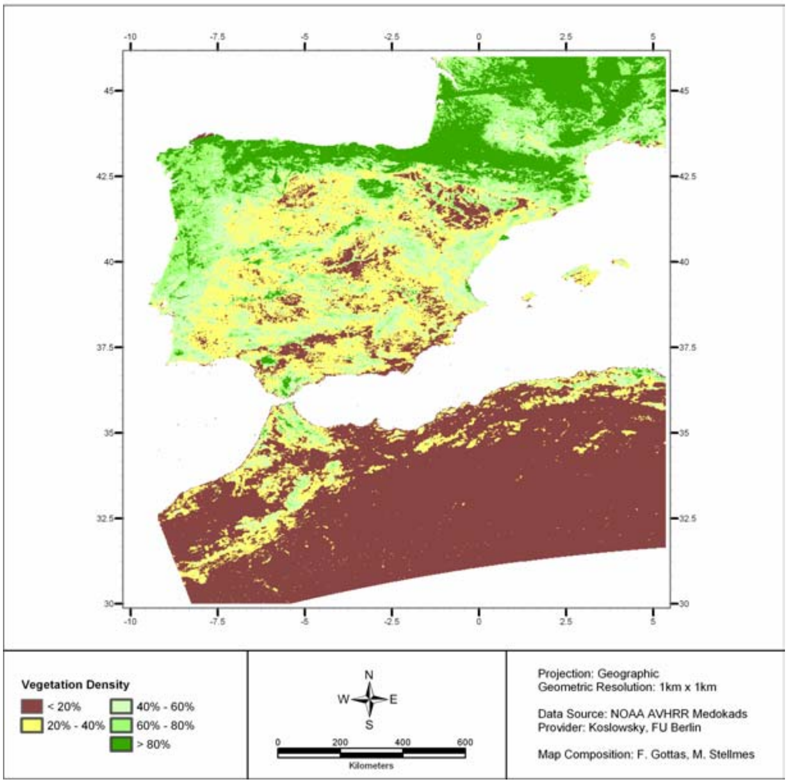

Figure 4: Vegetation density derived from the NOAA AVHRR MEDOKDAS dataset for April 1990 (above) and September 1990 (below).

In April almost the whole Iberian Peninsula is covered by vegetation. Only few areas show no or sparse vegetation. Good recognisable are the areas near Tortosa and Valencia, where rice is cultivated. In April these areas are still not vegetated (vegetation density < 20%). Areas used for agricultural purposes like Tierra the Campos were not yet harvested. Also the African Coast is mainly vegetated.

In September the situation changed. The harvest has finished and many areas are now sparsely vegetated or even completely uncovered. Only areas dominated by forest as the south of France and the Atlantic coast of Portugal and Spain, are densely vegetated. Also the rice cultivation areas show high vegetation densities (> 80%).

2.4 Land Cover Classification

Regarding the interpretation of the trend classes and the derived hot spots, it is important, as mentioned before, to take into consideration thematic layers like the land cover at different time steps. Furthermore, land cover information layers play also an important role for land degradation modelling.

Therefore a multi-temporal land cover classification was realized on the MEDOKADS dataset to create land cover maps for the years 1990 and 1998.

2.4.1 Pre-Processing

The classification was performed with a layerstack of a two years' period of monthly NDVI-data of the NOAA AVHRR MEDOKADS time series covering the Iberian Peninsula. The classification could also have been implemented on decades, which deliver a better temporal resolution. These data could describe the phenological cycle of the different land cover classes more detailed. But due to cloud artefacts and a highly variable sun-target-sensor-geometry the decadal data are very noisy. Since these effects were mainly eliminated through a Maximum Value Compositing, the monthly data were preferred for analysis.

2.4.2 Classification

In a first step an investigation was carried out to evaluate how many land cover classes can be differentiated with the 1-km-data data set. In comparison to the Corine Land Cover map 1990 (consisting of 44 classes), first of all for every Corine class the correspondend pixels of the NDVI-layerstack were masked out. Afterwards an unsupervised classification was carried out for every masked image of the NDVI-layerstack. Using the above mentioned procedure spectral subclasses of every land cover class should have been detected, but the subsequent supervised classification with the extracted signatures was not convincing.

The CLC classification is based on visual interpretation, where also texture parameters are considered. Explaining the poor results of the NDVI-based classification it has to be taken into consideration that for a classification of coarse data like the 1 km NDVI time series only spectral differences or the course of the signature respectively can be used to classify the land cover classes. Subsequently many classes of CLC can not be separated with the used dataset.

Separable classes and their typical signatures were attempted to extract by hierarchical clustering. This clustering was performed with the Pearson correlation coefficient and the cosines. These distance parameters have been chosen, because within every land cover class there was a high variability in the height of the NDVI values, but a high similarity in the course of the signatures which is taken into account by these distance measures. But even with the cluster analysis the assignment of the signatures to land cover classes was proved to be very difficult.

One major problem is that the NDVI values of many pixels are not only composed by one land cover class but by several different. Therefore, the signatures of these pixels are a mixture of these land cover classes. Thus, it is not possible to assign these signatures clearly to one class.

Besides, many classes, which are distinguished by Corine Land Cover, can not be separated at all, and therefore are merged to new classes. In contrary, some classes like for example 'rice' can be determined well, because the course of the NDVI is very characteristic and unique.

Water, rural areas and bar soil/rocks caused great difficulties. They all show a very low NDVI and no variability during the year. But because of their usually small spatial dimension, only few pixels exist which are really pure. If there is also vegetation in these areas, the vegetation superimposes the signature of these land cover classes and therefore the pixels are often assigned to sparse vegetation. Because urban areas and water bodies are very good classified in the Corine Land Cover, it was decided to use this information and mask them out in the multi-temporal classification.

2.4.3 Preliminary Results

The classification result for the year 1990 (fig. 5) shows in comparison to Corine Land Cover, that the structures of land cover are good recognizable for the majority of the Iberian Peninsula. Problems occur in the North-western part of the Peninsula, which is classified mainly as mixed forest. This area is dominated by a very heterogeneous land cover dominated by forest, which therefore can not be separated into different classes. Due to their specific signatures specialized cultivations like rice and fruits can be identified in most cases very well.

When interpreting the result, one problem is that Corine Land Cover can not be taken as a full reference. The major problem is, as mentioned before, that this information layer was build based on visual interpretation. In contrary, we can only rely on spectrally differences and the course of the NDVI over the year for the coarse resolution data. Therefore it does not seem advisable to compare directly the Corine Land Cover information layer to the results of the multi-temporal classification approach.

Another problem when classifying other years with the acquired signatures occurs caused by different phenological cycles between years. Thus, it is necessary to modify the signatures used for a supervised classification for two different time steps.

Further steps will be taken to improve the classification results. Additional information can be included. An improvement could be achieved using also reflectance values and other information layers, like i.e. the landscape structure, which affects the land cover and the phenological cycle. These approaches could help to eliminate or reduce intersections of land cover classes.

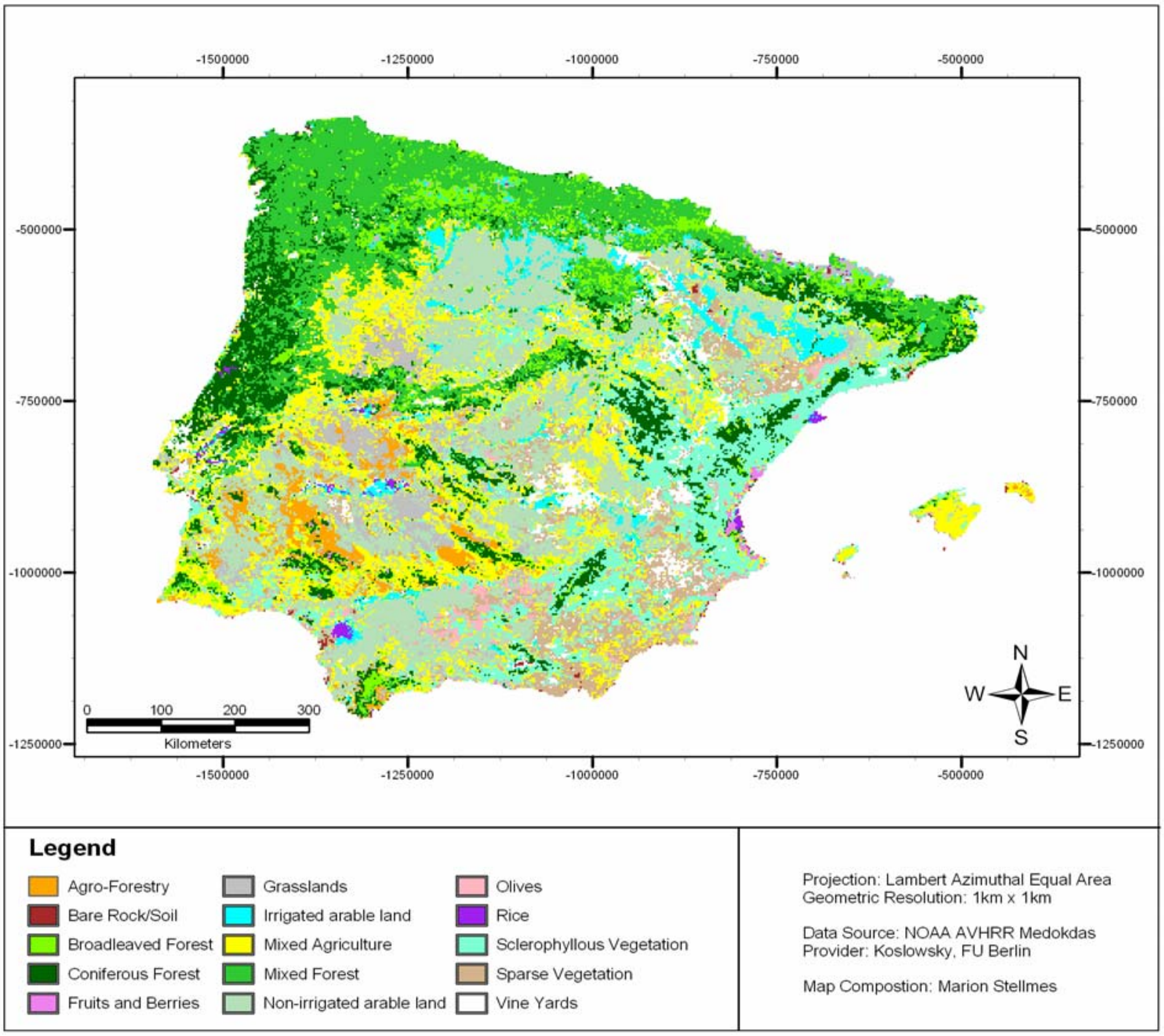

Figure 5: Multi-temporal land cover classification based on the NDVI of the NOAA AVHRR MEDOKDAS time series.

References:

Caselles, V. and Sobrino, J.A. (1989): Determination of frosts in orange groves from NOAA-9-AVHRR data. Remote Sensing of Environment, 29:135-146.

DeFries, R. S., Hansen, M., Townshend, J. R. G., and Sohlberg, R. (1998): Global land cover classifications at 8 km spatial resolution: the use of training data derived from Landsat imagery in decision tree classifiers. International Journal of Remote Sensing, 19(16):3141–3168.

European Commission (1998): An Integrated Approach to Assess and Monitor Desertification Processes in the Mediterranean Basin (DeMon-II). Final Report, Eurpean Comission, Directorate General Joint Research Center, Ispra, Contract No.: 11589-95-12 A2 FP ISP B

EPA (2000): Guidance for Data Quality Assessment - Practical Methods for Data Analysis. United States Environmental Protection Agency (EPA), Washington, DC 20460. EPA/600/R-96/084.

Erbrecht, Tim (2003): Monitoring of land degradation and land use systems with high temporal resolution remote sensing data. Unpublished diploma thesis. University of Trier.

European Commission (2002): Implementing the new EU Rural Development – The Spanish Case.
URL: http://europa.eu.int/comm/agriculture/rur/countries/es/case.pdf. [03.03.2003].

Hartung, J. (1995): Statistik: Lehr- und Handbuch der angewandten Statistik. R. Oldenbourg, München, 10th edition. Kok, K., Clavaux, M., Heerebout, W., and Bronsveld, K. (1995). Land degradation and land cover change detection using low-resolution satellite images and the CORINE database: a case study in Spain. ITC Journal, 3:217–228.

NASA (2002c): Pathfinder Data Set Product Notes.
URL: http://daac.gsfc.nasa.gov/campaign$_$docs/land$_$bio/checks.html, [14.08.2002].

Price, J.C. (1993): Estimating leaf area index from satellite data. IEEE Transactions on Geoscience and Remote Sensing, 31(3): 727-734.

Walker, G. (1999). Valencia 1999 report:

URL: http://www.ierm.ed.ac.uk/internal/valencia.htm. [03.03.2003].

WP3: Land degradation modelling

3.1 Approach

This work package is built on the rationale that: 1) dryland condition can be quantified in terms of the land's capacity to retain and utilise local water resources, 2) for given climate conditions the density or total phytomass of the vegetation that can be sustained at long timescales (i.e. years to decades) is primarily limited by soil moisture availability, and hence 3) observations of actual vegetation density can, when combined with relevant information on local climate conditions, be used to assess the relative importance of plant available moisture on the local water balance (Boer 1999).

During the reporting period we have explored modifications to the land degradation assessment procedure developed by Boer (1999), mainly to adapt the method to the coarse spatial resolution of the available data sets (i.e. 1-8 km). The current approach follows Boer (1999) by:

- quantifying land condition in terms of the capacity to retain and utilise local water resources
- using a reference function to predict potential vegetation density and the associated water balance from mean monthly precipitation (P) and potential evapotranspiration (E_0) at reference sites.
- assessing the actual water balance from the deviation between predicted potential and actually observed vegetation density.

We depart from the local water balance:

$$P - E_a - D - \Delta S = 0 \qquad \text{[eq. 1]}$$

where P is precipitation, E_a is actual evapotranspiration, D is drainage and ΔS is the change in the soil water store. At long time scales (i.e. decades), ΔS can be assumed to be small so that eq. 1 can be simplified to:

$$P - E_a - D = 0 \qquad \text{[eq. 2]}$$

The fraction E_a/P represents the water resources that are potentially available for primary production, whereas the water that drains from the site through percolation beyond the root zone or lateral (sub)surface flow (D/P), is essentially lost for local plant production. In the dry zones of Mediterranean Europe and other moisture-limited environments, the maximum vegetation density (V_{max}) corresponds to a situation where the vegetation thoroughly exploits the soil, drainage is minimised, and long-term E_a approaches long-term P:

$$\frac{E_a}{P} \rightarrow 1.0 \qquad \text{[eq. 3]}$$

Degraded land, characterised by deteriorated soil hydrological properties (Imeson 1986; Brandt and Thornes 1996; Boer 1999), loses some of its capacity to retain local water resources. It can therefore sustain less vegetation and its E_a/P will be smaller than 1.0. On irrigated land or in sites where runon accumulates E_a/P can exceed 1.0 (e.g. (Domingo et al. 2001). For large areas, such as the 64 km^2 grid cells used in the present study, E_a/P will normally not exceed 1.0. It is important to note that E_a/P can be smaller than 1 for other reasons than land degradation, for example in areas where the soil has an inherently low water holding capacity, such as on shallow sandy soils. To minimise erroneous assessments, we propose to use E_a/W_{max}, where W_{max} is the long-term maximum amount of plant available soil water, rather than E_a/P as an indicator of dryland condition because E_a/W_{max} must, by definition, be equal to 1.0 on non-degraded land.

Based on observations of evergreen perennial vegetation across Australia, (Specht 1972) developed a simple model for the assessment of E_a/W_{max} from monthly precipitation (P), potential evapotranspiration (E_0), and the maximum amount of plant available water that can be stored in the soil (S_{max}). In 'full-grown' communities on level terrain he observed a linear relationship between the monthly ratio of actual and potential evapotranspiration and the status of the plant available water store (W):

$$\frac{E_a}{E_0} = k.W \qquad \text{[eq. 4]}$$

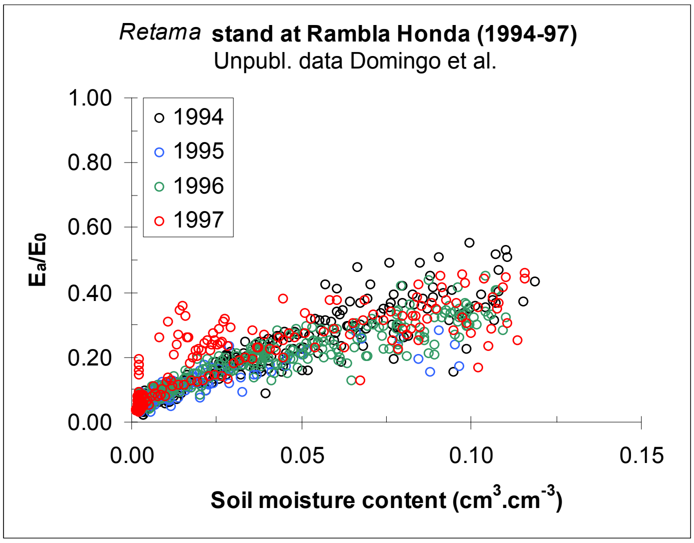

Figure 1: Observed ratio of actual and potential evapotranspiration in a Retama sphaerocarpa stand at Rambla Honda, Almería, SE Spain. Source: Unpubl. data F. Domingo & L. Villagarcía.

The slope of this curve, k, represents an evaporative coefficient that appeared to be highly stable through the year. A similar constancy of this relationship was observed in stands of evergreen shrubs (*Retama sphaerocarpa*) at the Rambla Honda Field site in SE Spain (Fig. 1) Unpubl. data F. Domingo & L. Villagarcía). The evaporative coefficient can be calculated by running equation 4 at monthly time steps until all plant available soil water is thoroughly used but never is completely depleted (Fig. 2). In Australia, k values range from less than 0.035 cm^{-1} in the arid zone, to 0.035-0.045 cm^{-1} and 0.045-0.055 cm^{-1} in the semi-arid and sub-humid zones, respectively (Specht and Specht 1989). The evaporative coefficient can be used as a topoclimatic moisture index, it is strongly correlated with Budyko's (1974) aridity index, E_0/P (Fig. 3, but is especially convenient for vegetation studies because it takes the seasonal distribution of precipitation and atmospheric moisture demand, as well as the soil water holding capacity, into account. It was found to be a reliable predictor of canopy density in

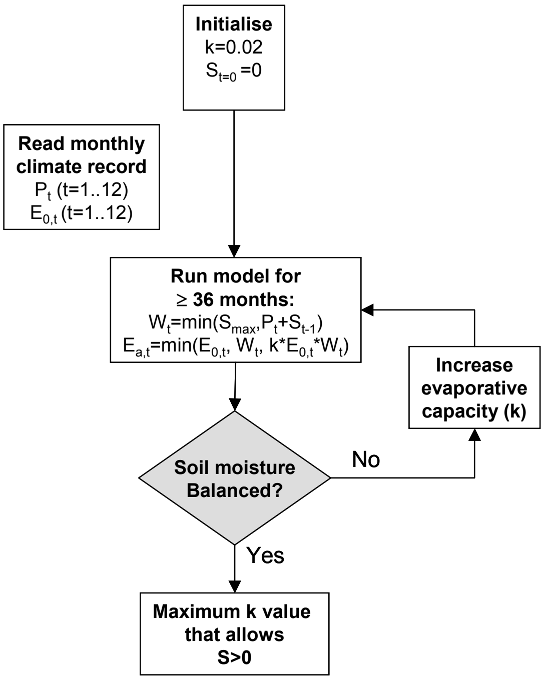

Figure 2: Iterative procedure for the calculation of the evaporative coefficient: P: monthly precipitation, E_0: potential evapotranspiration, S: plant available soil water store, S_{max}: maximum plant available soil water.

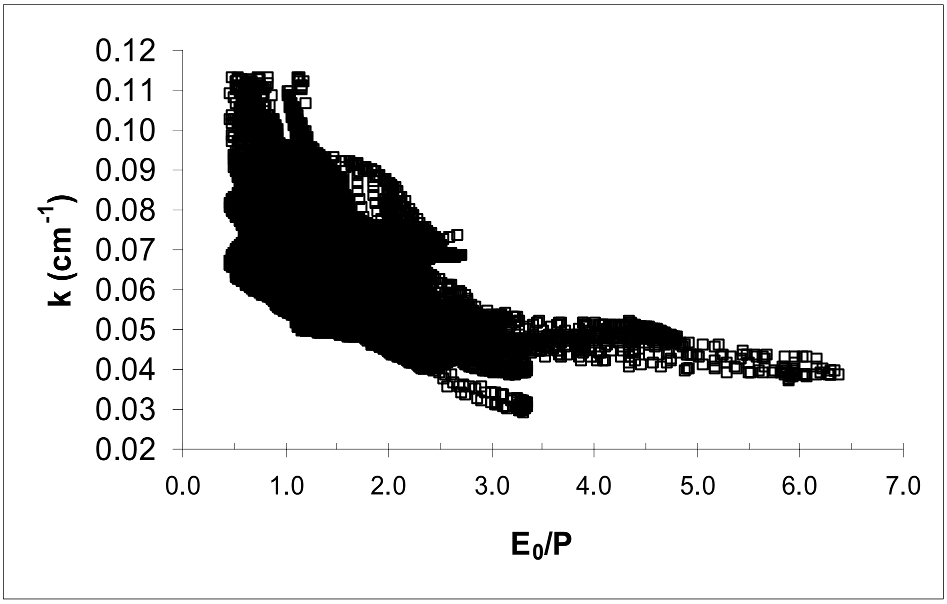

Figure 3: The relationship between the evaporative coefficient, k, and the aridity index, E_0/P in the LADAMER study area.

full-grown *Eucalyptus* communities across Australia and of potential values of the Normalised Difference Vegetation Index (NDVI) on Landsat TM imagery in SE Spain (Boer and Puigdefábregas 2003).

Specht's work offers several elements for the assessment of dryland condition in large study areas from remotely-sensed vegetation density. The evaporative coefficient that can be calculated and spatially distributed from existing data of monthly P and E_0, and soil water holding capacity, has shown some potential as a predictor of the climatic maximum vegetation density (V_{max}) in moisture-stressed environments (Specht and Specht 1989; Boer and Puigdefábregas 2003). If equation 4 can be shown to be acceptable as a general model of long-term water use by dryland vegetation on both undisturbed and degraded land, we can use non-degraded sites (i.e. $V \approx V_{max}$) with relatively arid climate and/or shallow soils (i.e. low k values) as spatial analogues of climatically more humid (i.e. high k values), but degraded, land (i.e. $V < V_{max}$), and assess monthly E_a/W for any grid cell as:

$$\frac{E_{aj}}{W_j} = k'.E_{0j} \qquad \text{[eq. 5]}$$

where E_{aj} and E_{0j} are actual and potential evapotranspiration for month j, W_j is the plant available water for month j, and k' is the evaporative coefficient that is predicted for that grid cell on the basis of its actual vegetation density (V) and inversion of the regional model $V_{max}=f(k)$.

A comparison of the summed monthly E_a/W with those of the reference situation, E_a/W_{max}, shows what fraction of the potentially available annual water resources is retained and utilised on site by the actual vegetation. Assuming that E_0 is independent of land condition at the kilometre scale, this fraction can be assessed as:

$$LCI = \frac{\sum k'.E_{0j}}{\sum k.E_{0j}} = \frac{k'}{k} \qquad \text{[eq. 6]}$$

where LCI is the land condition index, E_{0j} is the potential evapotranspiration for month j, and k and k' are, respectively, the calculated potential value and predicted actual value of the evaporative coefficient.

Below, we explore the practicality of this approach to land condition assessment and identify priorities for further research.

3.2 Material and methods

To run the proposed land condition assessment on the LADAMER study area we collected the following data set:

- A time-series (1981-2001) of monthly NOAA Pathfinder NDVI at 8 km spatial resolution,
- Spatially distributed estimates of mean monthly P and potential evapotranspiration (E_0) at 1 km resolution,
- Spatially distributed estimate of total soil water available to plants (W_{100}) in the top 100 cm of the soil at 1 km resolution.

The NOAA NDVI data were provided by The Remote Sensing Dept, Univ. Trier, while the climate surfaces (based on MARS data) and the W_{100} layer (derived from the European Soil Data Base, (European Soil Bureau 1999) were part of the GIS data set prepared for the PESERA Project ('Pan-European Soil Erosion Risk Assessment') by the Institut National de la Recherche Agronomique in Orléans, France, and the European Soil Bureau in Ispra, Italy. The NOAA NDVI data have been reprojected to the Lambert Azimuthal projection using IDRISI, and then resampled to an 8 km grid version of the LADAMER map frame. The other data layers only needed resampling to the 8 km grid.

For the current land condition assessment we have used 60 images of monthly NDVI covering the period of September 1996 to August 2001, roughly five hydrological years. Using the mean minimum NDVI of the 60 images (i.e. 115.2) as a reference, a time-integrated NDVI value (TINDVI) was computed from a summation of all positive differences between monthly NDVI values and the reference (Fig. 5):

$$\mathrm{TINDVI}_k = \sum \min(0, (\mathrm{NDVI}_{k,j} - \overline{\mathrm{NDVI}_{\min}})) \qquad \text{[eq. 7]}$$

where TINDVI_k is the time-integrated NDVI of grid cell k, $\mathrm{NDVI}_{k,j}$ is the mean NDVI of grid cell k for month j, and $\overline{\mathrm{NDVI}_{\min}}$ is the mean minimum NDVI for the images covering the period September 1996-August 2001. Time-integrated NDVI derived from NOAA-AVHRR imagery has been successfully used for assessing total phytomass, rain-use efficiency and land degradation at sub-continental scales (e.g. (Paruelo and Lauenroth 1995; Holm et al. 2003; Prince et al. 1998). Here we will use the TINDVI over 5 hydrological years as an index of the currently sustained vegetation density (i.e. V) and TINDVI_{max} as the maximum vegetation density (i.e. V_{max}) that can be sustained under current climate conditions.

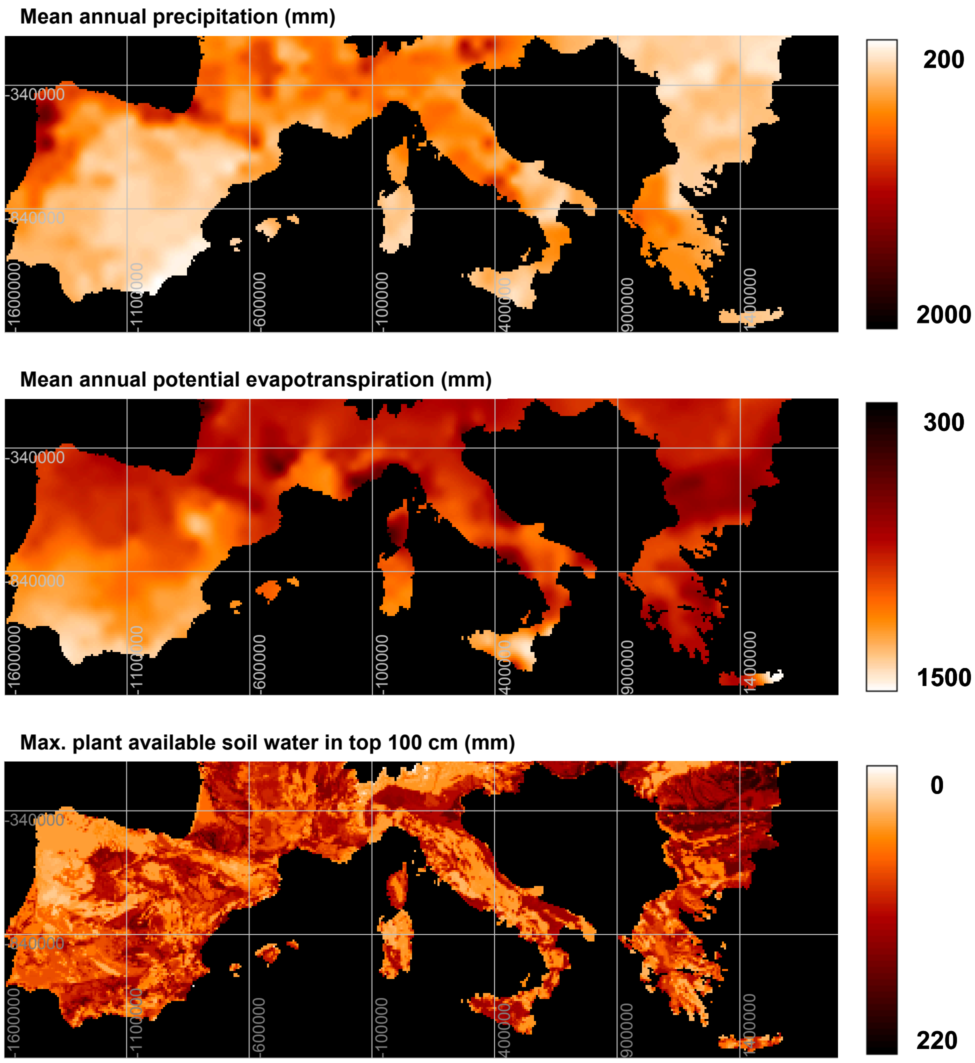

Figure 4: From top to bottom: mean annual precipitation, mean annual potential evapotranspiration and the maximum amount of plant available soil water in the top 100 cm of the soil.

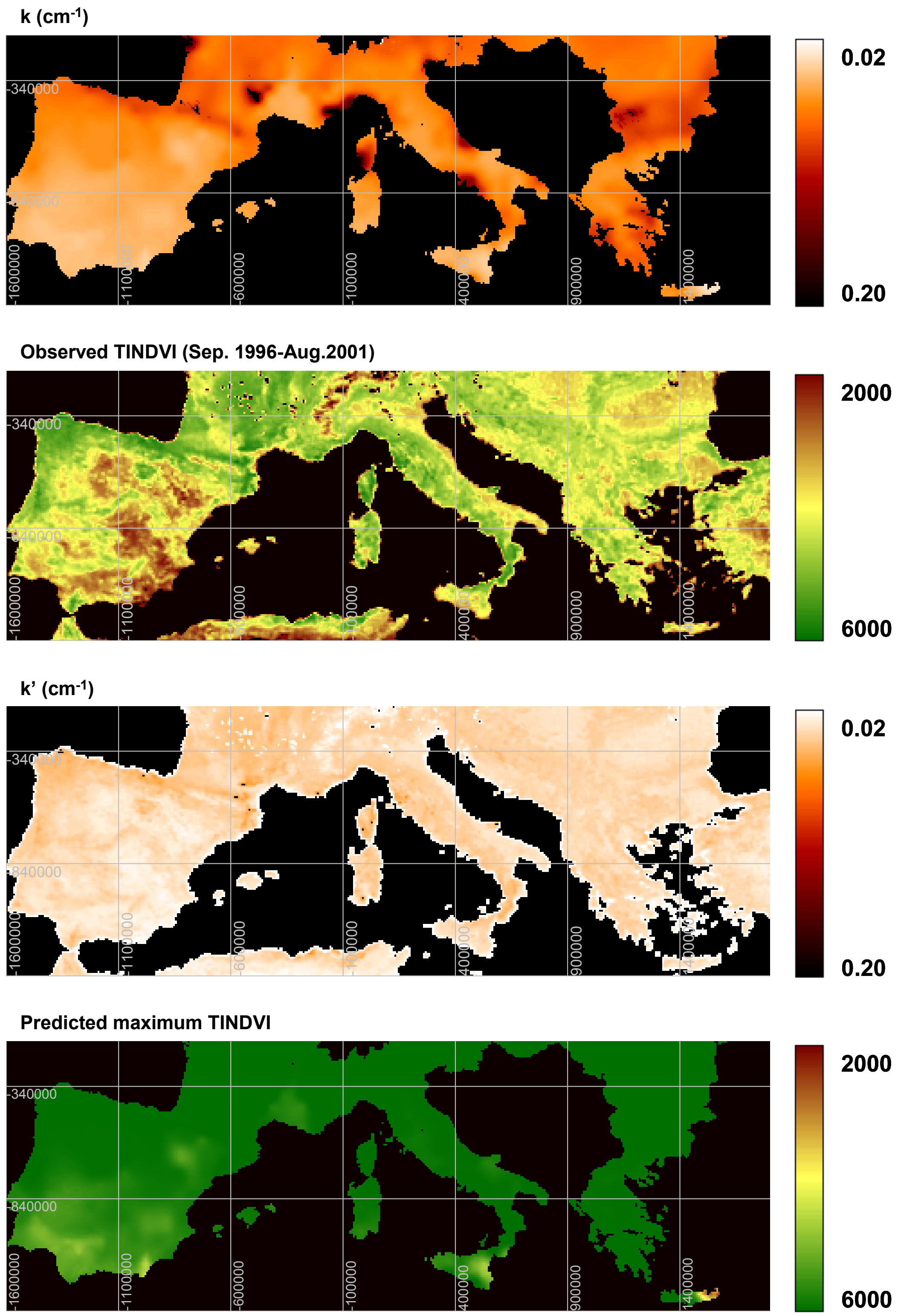

Figure 5: From top to bottom: the evaporative coefficient, k, observed time-integrated NDVI (Sep. 1996-Aug.2001), predicted evaporative coefficient, k', and predicted maximum time-integrated NDVI.

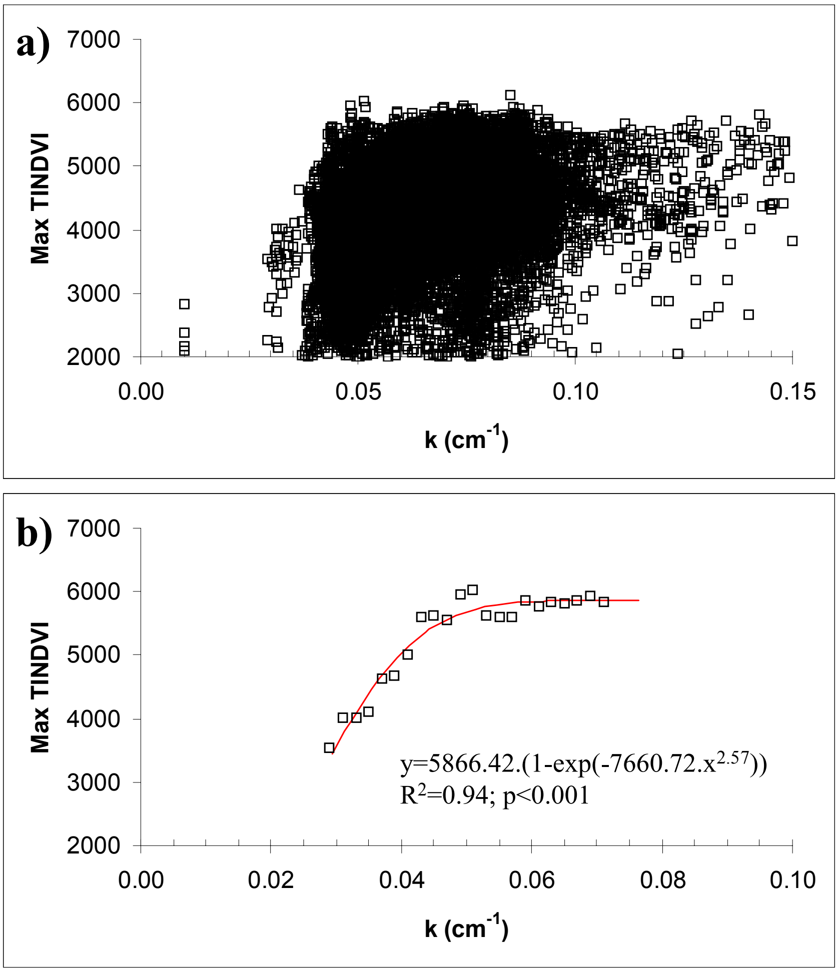

Figure 6: Scattergram of observed time-integrated NDVI (Sep.1996-Aug.2001) against the evaporative coefficient k (a). Data points and fitted curve that define the upper boundary of the k-TINDVI data envelop for grid cells with moisture-stressed environments (b).

The data layers of mean monthly P and E_0, and W_{100} were used to calculate the evaporative coefficient (Fig. 4,) according to the iterative procedure depicted in Figure 2). Resulting values range from 0.031 cm^{-1} in the eastern part of Crete to more than 0.10 cm^{-1}in humid coastal areas. Since our approach is designed for moisture-stressed environments we will focus on grid cells with an aridity index greater than 1.0, roughly corresponding to k values smaller than 0.06 cm^{-1}.

A scattergram of TINDVI as a function of the evaporative coefficient, k, shows a data cloud with a rather clearly defined upper margin (Fig. 6a). After calculating maximum TINDVI values for 36 intervals of 0.002 k units in the k range of 0.03-0.07 cm^{-1} an exponential function was fitted through all data points with an aridity index greater than 1.0 (n=23):

$$TINDVI_{max} = a.(1 - \exp(-b.k^{c})) \qquad \text{[eq. 8]}$$

where $TINDVI_{max}$ is the maximum TINDVI observed in a small k interval, k is the calculated value of the evaporative coefficient for the grid cell with the greatest TINDVI in a given k interval, and a, b, and c are constants (Fig. 6b). A map of predicted $TINDVI_{max}$ is shown in Figure 5.

By inversion of equation 8 we obtain an expression for the prediction of the evaporative coefficient, k', corresponding to the actual value of TINDVI (Fig. 5):

$$k' = \left[\frac{-1}{b} * \ln\left(\frac{-\text{TINDVI}}{a} + 1 \right) \right]^{1/c} \qquad \text{[eq. 9]}$$

Finally, the land condition index is obtained by calculating the ratio k'/k (Fig. 7).

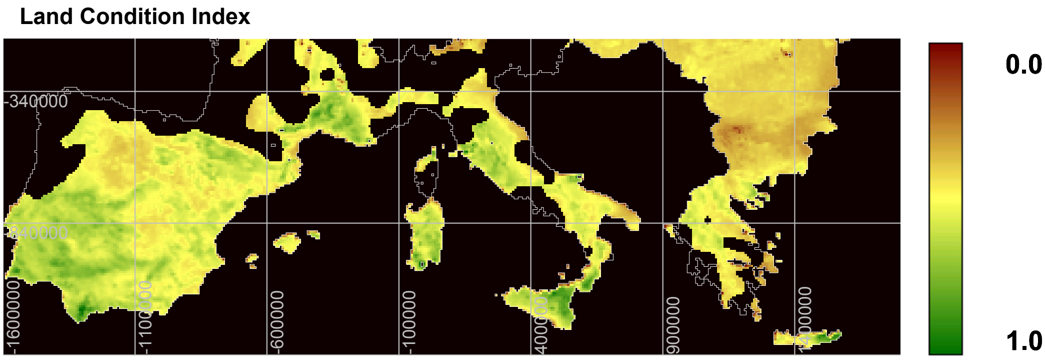

Figure 7: Land Condition Index for all grid cells with aridity index greater than 1.0.

3.3 Discussion of results

Figure 7 shows the spatial distribution of the land condition index in Mediterranean Europe. The map quantifies the fraction of the actual and maximum amount of plant available soil water that is retained and utilised on site by the current vegetation mass. According to this assessment, large areas of land in relatively poor condition (brown tones) are found, for example, in Castilla-Leon and Castilla-La Mancha (Central Spain), Roussillon in France, Apulia in Southern Italy and in Northern Greece. Large areas of land in relatively good condition (green tones) are identified in mountainous areas of the Iberian Peninsula, Provence in SE France, eastern Sicily and the eastern part of Crete. A visual comparison with the Corine Land Cover map indicates that the land in poor condition is especially abundant in areas of rainfed agriculture, whereas land in relatively good condition is frequent in areas dominated by shrub or forest vegetation. From a soil hydrological point of view this pattern makes good sense, of course, since dynamic soil properties, such as organic matter content and aggregate stability that are used as indicators of the 'health' of the soil e.g. (Herrick et al. 2001) are known to be negatively affected by many forms of agricultural land use e.g. (Cammeraat and Imeson 1998). A single assessment for the entire LADAMER study area implies that the condition of all grid cells is quantified according to a single scale. The LCI scale, however, is derived from the relationship between the evaporative coefficient and the maximum TINDVI values in the study area, which are typically observed in forested areas or other land with semi-natural vegetation. This explains the abundance of relatively low LCI values for the LADAMER study area as a whole (i.e. median LCI=0.54). More subtle differences in condition among grid cells of the same land use cannot be readily appreciated on the current LCI map. Such information can be obtained to some extent by analysing the frequency distributions of LCI per Corine Land Cover class (i.e. upcoming work), or preferably by applying the proposed assessment procedure separately on each land use class.

The proposed approach to land condition assessment uses a set of existing data layers, is objective and reproducible, and is conceptually sound with current ecological understanding of dryland degradation. It obviously requires further development, testing, and verification. Priorities for further research work include:

- verification and, if required, modification of equation 4 as a general model for long-term water use by natural vegetation and rainfed agricultural crops in dryland environments.
- collection and analysis of (existing) data on the relationship between long-term vegetation density, dynamic soil hydrological properties, and the land's capacity to retain and utilise local precipitation.
- assessment of the accuracy of existing input data layers, especially the maps of mean monthly precipitation (Fig. 8)
- assessment of the accuracy of time-integrated NDVI as an index of total 'actively transpiring' phytomass, and the testing of alternative indices, for example, based on the surface infrared temperature – NDVI data space e.g. (Gillies et al. 1997; McVicar et al. 2000; Sandholt et al. 2002).

Relative difference in mean annual precipitation

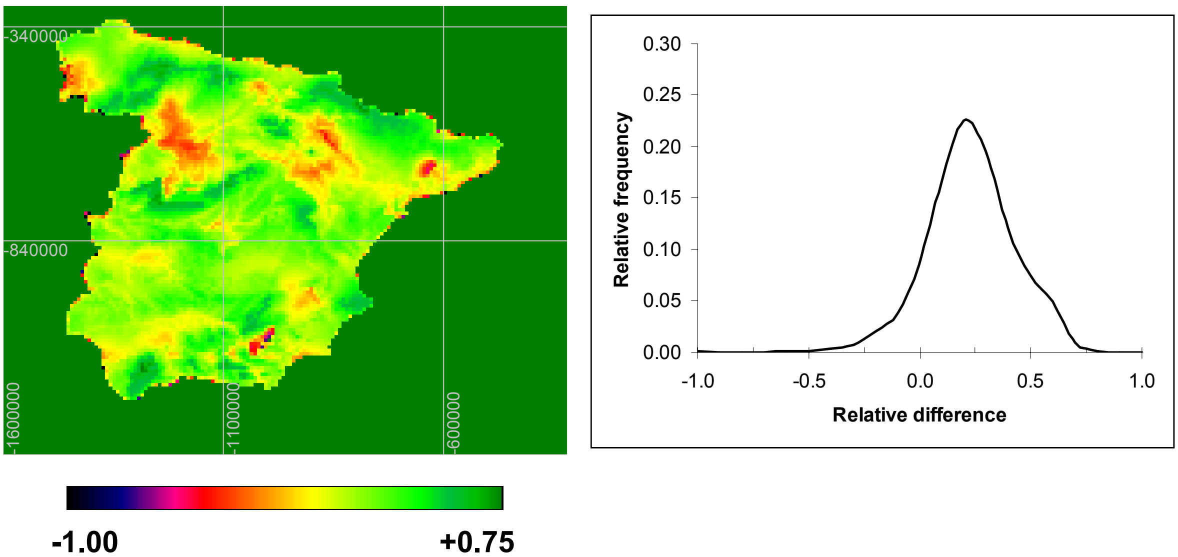

Figure 8: Relative difference (Left) between two maps of mean annual precipitation over the Spanish part of the Iberian Peninsula, calculated as: (MAP1-MAP2)/MAP1. MAP1 refers to a resampled version of spatially distributed estimates of mean annual precipitation by the Spanish Government (Sanchez Palomares et al. 1999); MAP2 refers to the data layer used in the present study that was based on MARS data. Right: frequency distributions of the relative differences in mean annual precipitation, showing a general underprediction by the map derived from the MARS data (MAP2).

References:

Boer, M. M. (1999) Assessment of dryland degradation: linking theory and practice through site water balance modelling. Dissertation Dept. Phys. Geography, Utrecht University, Utrecht, The Netherlands.

Boer, M. M. and Puigdefábregas, J. (2003). Predicting potential vegetation index values as a reference for the assessment and monitoring of dryland condition. - International Journal of Remote Sensing 24: 1135-1141.

Brandt, J. and Thornes, J. B. (Eds.) (1996). Mediterranean desertification and land use. - John Wiley & Sons Ltd.

Budyko, M. I. (1974). Climate and life. - Academic Press.

Cammeraat, L. H. and Imeson, A. C. (1998). Deriving indicators of soil degradation from soil aggregation studies in southeastern Spain and southern France. - Geomorphology 23: 307-321.

Domingo, F., Villagarcía, L., Boer, M. M. and Puigdefábregas, J. (2001). Evaluating the long-term water balance of arid zone stream bed vegetation using evapotranspiration modelling and hillslope runoff measurements. - J. Hydrol. 243: 17-30.

European Soil Bureau. (1999) European soil database version 1.0. 1999. European Soil Bureau, European Commission.

Gillies, R. R., Carlson, T. N., Cui, J., Kustas, W. P. and Humes, K. S. (1997). A verification of the 'triangle' method for obtaining surface soil water content and energy fluxes from remote measurements of the Normalized Difference Vegetation Index (NDVI) and surface radiant temperature. - International Journal of Remote Sensing 18: 3145-3166.

Herrick, J. E., Whitford, W. G., De Soyza, A. G., Van Zee, J. W., Havstad, K. M., Seybold, C. A. and Walton, M. (2001). Field soil aggregate stability kit for soil quality and rangeland health evaluations. - Catena 44: 27-35.

Holm, A. M., Cridland, S. W. and Roderick, M. L. (2003). The use of time-integrated NOAA NDVI data and rainfall to assess landscape degradation in the arid shrubland of Western Australia. - Remote Sensing of Environment 85: 145-158.

Imeson, A. C. (1986). An eco-geomorphological approach to the soil degradation and erosion problem. - In: Fantechi, R. and Margaris, N. S. (eds.), Desertification in Europe. Proceedings of the Information Symposium in the EEC Programme on Climatology, held in Mytilene, Greece, 15-18 April 1984. Reidel Publishing Company, pp. 110-125.

McVicar, T. R., Jupp, D. L. B. and Bierwirth, P. N. (2000). Regional ecohydrological indices: monitoring moisture availability and drought in Australia and Papua New Guinea. - In: McVicar, Tim R. (ed.), Proceedings of the Land EnvSat Workshop, 10th Australasian Remote Sensing and Photogrammetry Conference, Adelaide, 25 August 2000. CSIRO Land and Water, pp. 1-14.

Paruelo, J. M. and Lauenroth, W. K. (1995). Regional patterns of Normalized Difference Vegetation Index in North American shrublands and grasslands. - Ecology 76: 1888-1898.

Prince, S. D., Brown De Colstoun, E. and Kravitz, L. L. (1998). Evidence from rain-use efficiencies does not indicate extensive Sahelian desertification. - Global Change Biology 4: 359-374.

Sanchez Palomares et al. (1999) Modelos y cartografia de estimaciones climaticas para la España peninsular. MAPA, INITAA, Madrid.

Sandholt, I., Rasmussen, K. and Andersen, J. (2002). A simple interpretation of the surface temperature/vegetation index space for assessment of surface moisture status. - Remote Sensing of Environment 79: 213-224.

Specht, R. L. (1972). Water use by perennial evergreen plant communities in Australia and Papua New Guinea. - Australian Journal of Botany 20: 273-299.

Specht, R. L. and Specht, A. (1989). Canopy structure in Eucalyptus-dominated communities in Australia along climatic gradients. - Acta Oecologica 10: 191-213.

WP4 – Land use change modelling

Abstract

The two main activities of RIKS in the Ladamer project are related to land use modelling and calibration/validation methods. For the land use modelling there has been progress both on the macro- and the micro level land use modelling. For the calibration and validation task the focus has been on the development of goodness-of-fit measures for cellular models.

Macro level land use modelling

The macro level models operate at the NUTS 2 level they set the socio-economic environment for land use change at the cellular level. The main function of the macro models is to give a good prediction of the socio-economic status for each region in the model at different moments in the future. These predictions are based on scenarios that give the nationwide trends in time and historical data from the EUROSTAT REGIO database.

Different variations of four types of models that are found in the literature are considered:

- Constant share model
- Shift share model (14 variations)
- Single constrained gravity model (2 main variations)
- Double constrained gravity model (2 main variations)

Furthermore, a new densification model has been developed. The densification module intends to predict land use claims (acreages of land for different land use types) this module functions as an intermediate between the macro model and the micro model. The macro model produces results in the form of socio-economic figures (employment and population), whereas the micro model takes land use acreages as input. The new model is based upon a continuous equilibrium of land use pressure.

Micro level land use modelling

At the micro level of Ladamer a model is applied that has been used before in other EU projects (Moland, Murbandy, Medaction) it is the Constrained Cellular Automata (CCA). A characteristic of the CCA is that it uses many parameters, especially for the calculation of the neighbourhood effect. The large amount of parameters may be an obstacle in the calibration process. In order to reduce the complicatedness and to ease calibration the number of parameters in the Ladamer model will be reduced. This is possible by restricting the possible curves of the Neighbourhood Rules to composite exponential curves. First experiments with the reduce set of parameters yield possible results and two conclusions:

1. The reduced parameter set can substitute the original full parameter set without compromising the model quality.
2. With the reduced parameter set the calibration of the model can be faster and more intuitive.

For the cellular model it is necessary to have a land use / land cover map at a 1 km resolution. For this purpose the Corine dataset has been aggregated from the 250m grid to a 1000m grid.

For this operation an aggregation algorithm has been developed that preserves the area taken in by each category for each region on the map. The reason applying this algorithm is that in a standard rescaling operation where a “majority gets all” rule is applied, often the presence of less prevalent or the more scattered categories will be reduced in this operation. The results of the aggregation differ wildly with the aggregation performed by ArcView (overlap +/- 50%), which calls for further evaluation.

Goodness-of-fit measures

The state of the art of evaluation of goodness-of-fit for cellular models involves the cell-by-cell pair wise comparison of model result versus ground truth map and derived statistics. The derived statistics are based upon the correspondence matrix. A reserve against these methods is that they fail to acknowledge two main characteristics of cellular models.

1. Cellular models are spatial. The cell-by-cell pair wise comparison ignores the spatial coherence found in cellular maps. Proximity relations are ignored, as are patterns such as clusters and contiguity
2. Cellular models are dynamic. By comparing result maps with reality it is ignored that cellular models are dynamic, evaluating the models should mean evaluating the dynamic behaviour of the model, above comparing the static outcomes of it.

To better evaluate model performance two comparison techniques are developed. The first comparison technique is the Fuzzy Set map comparison assesses map similarity while considering proximity relations and categorical similarity. The second technique is State-Space map comparison. This method aims to compare the nature of transitions that are found in two temporal series of maps.

4.1 Land use modelling

On the basis of a constrained cellular automata representation, an integrated land use model will be developed representing land use changes in the linked socio-economic, ecological and physical systems.

The processes will be represented at a high level of abstraction and the model will operate, at the least initially, at 2 coupled geographical levels:

(1) a ***macro level*** represented by the NUTS 2 administrative regions, and

(2) a ***micro-level*** represented by a cellular grid with a 1 km resolution.

A densification module functions as an intermediate between the macro level model and the micro level model. It “translates” the output of the macro level model (employment figures and population) to the input for the micro level model (acreages of land for different land use functions)

4.1.1 Macro level models

The macro level models operate at the NUTS 2 level they set the socio-economic environment for land use change at the cellular level. The main function of the macro models is to give a good prediction of the socio-economic status for each region in the model at different moments in the future. These predictions are based on scenarios that give the nationwide trends in time and historical data from the EUROSTAT REGIO database.

Different types of model are found in the literature. The main distinction is between process based models and statistic based models. Different models are implemented and evaluated against criteria relevant to Ladamer.

Different variations of four types of models are considered:

- Constant share model
- Shift share model
  - Constant relative shift
  - Constant absolute shift
  - Dynamic relative shift polynomial fit (1 - 3rd order)
  - Dynamic absolute shift polynomial fit (1 - 3rd order)
  - Dynamic relative shift time series regression (1 - 3rd order)
  - Dynamic absolute shift time series regression (1 - 3rd order)
- Single constrained gravity model
  - Attraction based upon accessibility (or potential)
  - Attraction based upon presence (or potential)
- Double constrained gravity model
  - Attraction based upon accessibility
  - Attraction based upon presence

Furthermore, a new densification model has been developed. The densification module intends to predict land use claims (acreages of land for different land use types) this module functions as an intermediate between the macro model and the micro model. The macro model produces results in the form of socio-economic figures (employment and population), whereas the micro model takes land use acreages as input.

4.1.1.1 Constant Share Model

The constant share model is the most straightforward model for regional distribution of super-regional or national trends. The model applies the national growth rate for each sector on every region.

$$A_{i,s}^{t} = G_s * A_{i,s}^{t-1} \quad (1)$$

$$G_s = \frac{A_s^t}{A_s^{t-1}} \quad (2)$$

Where:

$A_{i,s}^{t}$ Activity in region *i* and sector *s*

A_s^t Total activity in sector *s*

G_s National growth of sector *s*

4.1.1.2 Shift-Share Models

An alternative to the constant share model is the shift-share model. The main idea of the shift-share models is that the growth is not proportional but that the more competitive have a larger growth then the less competitive regions. The competitiveness of a region is calculated based upon empirical data.

There are different variations of shift-share models. There is difference in the way competitiveness in the past is calculated. It is based either on relative or an absolute growth. There are also several way to predict the current competitiveness of a region. Most common is to assume constant competitiveness. This means that for a recent year the competitiveness is calculated, and consequently extrapolated to the future.

Alternatively, for a range of years the competitiveness is calculated, the future competitiveness is then calculated on the basis of time-series analysis and extrapolation.

Calculation of competitiveness

Two kinds of competitiveness are recognized, competitiveness of the region and competitiveness of the sector. Since the development of the sector is given as a scenario, it is the competitiveness of the region that we are interested in.

The index of regional competitiveness is comparing the national growth, the growth per sector and the regional growth.

$$c_{ij} = n_{ij} + m_{ij} + r_{ij} \quad (3)$$

$$c_{ij} = E_{ij}^{t} - E_{ij}^{t*} \quad (4)$$

$$n_{ij} = E_{ij}^{t*} g \quad (5)$$

$$m_{ij} = E_{ij}^{t*} \left(g_i - g \right) \quad (6)$$

$$r_{ij} = E_{ij}^{t*} \left(g_{ij} - g_i \right) \quad (7)$$

The growth rates are given by:

$$g = \frac{\sum_{i,j} E_{ij}^{t} - \sum_{i,j} E_{ij}^{t*}}{\sum_{i,j} E_{ij}^{t*}} \tag{8}$$

$$g_i = \frac{\sum_{j} E_{ij}^{t} - \sum_{j} E_{ij}^{t*}}{\sum_{j} E_{ij}^{t*}} \tag{9}$$

$$g_{ij} = \frac{E_{ij}^{t} - E_{ij}^{t*}}{E_{ij}^{t*}} \tag{10}$$

Where E_{ij} stands for employment in sector *i* and region *j*.

A sectoral and a regional effect are calculated as:

$$m_j = \frac{\sum_i m_{ij}}{\sum_i E_{ij}^{t*}} = \frac{\sum_i E_{ij}^{t*}\left(g_i - g\right)}{\sum_i E_{ij}^{t*}} \tag{11}$$

$$r_j = \frac{\sum_i r_{ij}}{\sum_i E_{ij}^{t*}} = \frac{\sum_i E_{ij}^{t*}\left(g_{ij} - g_i\right)}{\sum_i E_{ij}^{t*}} \tag{12}$$

In the analysis, the growth of a region (employment) is defined as follows:

Growth equals national growth + regional advantage + industrial mix advantage. Since the growth of the sectors is given in the form of scenarios, it is the regional effect r_j that we are interested in.

Extrapolation methods

Three methods of extrapolation are applied. constant shift, polynomal curve fitting and linear regression on time series

4.1.1.3 Double Constrained Static Gravity Model

The static gravity model distributes national figures of land use acreage over the regions. The model is double constrained because both the total acreage per region and the acreage per land use type are predetermined. In order to apply the model it is necessary that the national socio-economic (population, employment) figures be expressed as land use claims (acres).

The model distributes the land use initially proportional to the attraction of each region for all land uses. Calibration factors per region and per land use type are applied to meet the constraints.

$$L_{r,s} = a_r * b_s * A_{r,s} \tag{13}$$

The constraints are expressed as follows:

$$R_r = \sum_s L_{r,s} \tag{14}$$

$$S_s = \sum_r L_{s,r} \tag{15}$$

Consequently the following input requirement must hold as well:

$$\sum_s \mathrm{S}_s = \sum_r R_r \tag{16}$$

Whereby:

$L_{r,s}$	Land use of sector *s* in region *r*
a,b	Balancing factors for regions and sector *s*
$A_{r,s}$	Attraction of region *r* on sector *s*
R_r	Area taken in by region *r*
S_s	Area taken in by sector *s*

Index for attraction of each region can be calculated as a function of the activity in each sector found in each region at the previous time step. See also the paragraph "single constraint dynamical gravity model".

National figures for activity are expressed as land claims by applying the densification module.

4.1.1.4 Single Constrained Dynamic Gravity Model

Relocation in each sector is modelled according to the following equation:

$$T_{i,j} = a_i * b_j * O_i * D_j * f\left(c_{i,j}\right) \tag{17}$$

$T_{i,j}$	amount of relocation of activity from region *i* to region *j*
O_i	total amount of relocation from region *i*
D_j	index of attraction of region *j*
$c_{i,j}$	distance between region *i* and *j* as generalized cost
$f\left(c\right)$	function on distance, *f* decays with distance

a_i and b_j are balancing factors, they are calculated iteratively to match the following constraints:

$$\sum_j T_{i,j} = O_i \tag{18}$$

$$Min_j \le \sum_i T_{ij} \le Max_j \tag{19}$$

The use of *Min* and *Max* make the model technically double-constrained, but because these represent an external policy option rather than the autonomous model dynamics the model is still conceptually a single constraint model (but within limits).
A fixed fraction ∂ of activity in every region is assumed not to relocate

$$O_i = (1-\partial) A_i \quad (20)$$

The activity at the next time step is thus calculated as:

$$A_j^{t+1} = A_j^t - O_j + \sum_i T_{i,j} \quad (21)$$

The index of attraction is calculated as a function of:

1. The activity (A) in the region in all sectors
2. The accessibility (P) of the region for/by activity in all sectors
3. Variables (X) exogenous to the module:
    a. Physical suitability
    b. Desertification
    c. Zoning
    d. Neighbourhood influence
    e. Random factor

The accessibility is calculated by means of a potential function:

$$P_i = \sum_j \left(A_j * f_{daily}\left(c_{ij}\right)\right) \quad (22)$$

f_{daily} function on distance, decays with distance

f_{daily} is generally not equal to f, because f represents the impact of distance relocating behaviour, whereas f_{daily} is about daily transport patterns.

For the calculation of the regional index of attraction several models are to be considered:

$$D_{A,j} = \sum_s \left(w_s^a * A_s + w_s^p * P_s \right) + \sum_r w_r^x * X_r \quad (23)$$

$$D_{B,j} = \sum_s \left(w_s^a * e^{A_s} + w_s^p * e^{P_s} \right) + \sum_r w_r^x * e^{X_r} \quad (24)$$

$$D_{C,j} = \prod_s \left(A_s^{w_s^a} * P_s^{w_s^p} \right) * \prod_e X_e^{w_e^x} \quad (25)$$

$$D_{D,j} = \prod_s \left(e^{w_s^a * A_s} * e^{w_s^p * P_s} \right) * \prod_n \left(e^{w_n^x * X_n} \right) = e^{\sum_s \left(A_s * w_s^a + P_s * w_s^p \right) + \sum_e X_e * w_e^x} \quad (26)$$

The advantage of the second and fourth model is that by the exponential functions have the appropriate domain [-∞, +∞] and range [0, +∞] and thus deal better with negative numbers than the third and fourth. D must be a positive value.

Besides regional relocation we also want to model the regional effect of national growth.

The regional trend is assumed to be a combination of the proportional national trend and the influence of regional advantages. In case of a positive trend attractive regions will grow more then less attractive regions; in case of a negative trend, attractive regions will decline less than less attractive regions.

The following equation is applied:

$$G_r = \frac{G * D_i^G}{\sum_i D_i^G} \tag{27}$$

Whereby again there are four methods available for combining factors:

$$D_{A,i}^G = w^P * A_i + Sign(G) * w^r * D_i \tag{28}$$

$$D_{B,i}^G = w^P * e^{A_i} + Sign(G) * w^r * e^{D_i} \tag{29}$$

$$D_{C,i}^G = A_i^{w^P} * D_i^{Sign(G) * w^r} \tag{30}$$

$$D_{D,i}^G = e^{w^P * A_i + Sign(G) * w^r * D_i} \tag{31}$$

$$Sign(G) = \begin{cases} G > 0 \rightarrow +1 \\ G \leq 0 \rightarrow -1 \end{cases} \tag{32}$$

Two different functions for *f* are supported:

$$f_A(d) = e^{-\alpha * d} \tag{33}$$

$$f_B(d) = d^{-\alpha} \tag{34}$$

4.1.2 Densification Module

A new model for densification has been developed which is based upon the notion of land use pressure. All land use types are assumed to exert pressure on each other. The model is an equilibrium model meaning that a every moment in time all land uses exert an identical pressure (but this pressure changes over time). The pressure of a land use is based upon its density and a pressure coefficient, whereby a higher pressure coefficient signifies a lower land use pressure. Changes in land use pressure affect both the density and the pressure coefficient, in a constant ratio which is called the elasticity (E) of the land use. (A very elastic land use reflects all change in a changing density whereas a non-elastic land use reflects changing pressure by adjusting the pressure coefficient thus without changing the density).

Even though an expanding area of land for a certain landuse is the result of increased activity this thus not necessarily mean that the new land has a higher density than the previous existing land. On the contrary, it is often found that newly taken in land has a lower density than the pre-existing land. This is reflected in the model by a relaxation factor (R) by an decrease in the pressure coefficient this means that at is present in the model is that new area of a land use is less dense then existing area of the same land use. This is expressed in a relaxation coefficient, which adjust the pressure coefficient according to change in acreage.

The following section gives a mathematical description of the model

4.1.2.1 Mathematical description of densification module, without relaxation factor

The model can be expressed mathematically in a system of second order polynomial equations, which can be solved numerically.

The aim of the densification module is to find land acreages (L) for every land use type *i* given land activities (A) for every land use type.

The total land use is fixed and adds up to 1:

$$\sum_i L_i = 1 \tag{1}$$

Every land use exerts land use pressure, relates to the density via a pressure coefficient:

$$P_i = \frac{A_i}{p_i L_i} \tag{2}$$

The land use pressure is in equilibrium, meaning that every land use exerts the same pressure.

$$P_i = P_j \tag{3}$$

The acreage depends on the acreage in the previous time step; likewise the pressure coefficient depends on the coefficient in the previous time step.

$$\begin{aligned} L^t &= L^{t-1} * x \\ p^t &= p^{t-1} * x_c \end{aligned} \tag{4}$$

The land use responds to pressure in by adjusting L and/or c. The balance of both is fixed and is called the elasticity E.

$$\begin{aligned} x_{p,i} - 1 &= E_i \left(x_i - 1 \right) \\ x_{p,i} &= E_i x_i + (1 - E_i) \end{aligned} \tag{5}$$

$$P_i = \frac{A_i}{p_i^{t-1} \left(E_i x_i + (1 - E_i) \right) x_i L_i^{t-1}} = \frac{A_i}{p_i^{t-1} L_i^{t-1} (1 - E_i) x_i + p_i^{t-1} L_i^{t-1} E_i (x_i)^2} \tag{6}$$

$$a_i = \frac{p_i^{t-1} L_i^{t-1} E_i}{A_i}$$
$$b_i = \frac{p_i^{t-1} L_i^{t-1} (1 - E_i)}{A_i} \quad (7)$$

$$\frac{1}{P_i} = \frac{1}{P_0} \quad (8)$$

$$a_i x_i^2 + b_i x_i = a_0 x_0^2 + b_0 x_0 \quad (9)$$

All can be expressed in the following set of equations:

$$F_0(x) = \sum L_i x_i - 1 = 0 \quad (10)$$

$$F_i(x) = a_i x_i^2 + b_i x_i - a_0 x_0^2 - b_0 x_0 = 0 \quad (11)$$

This system of equations can be solved numerically, with use of the Jacobean (J)

$$J = \begin{bmatrix} L_0 & L_1 & \cdots & L_n \\ -2a_0 x_0 - b_0 & 2a_1 x_1 + b_1 & \cdots & 0 \\ \vdots & \vdots & \ddots & \vdots \\ -2a_0 x_0 - b_0 & 0 & \cdots & 2a_n x_n + b_n \end{bmatrix} \quad (12)$$

4.1.2.2 First results and inclusion of relaxation factor

A region in the Netherlands (Arnhem agglo) during the period 1970-1996 serves as a test case. The aim of the test is to reproduce the change in land use acreage given the change in activity levels by calibrating the elasticity values. The calibration was not successful. The reason most probably is the assumption underlying equation 5, being that an expansion in area is always coupled to an increase in c. In reality it may be that an expansion in area may even be coupled to a reduction in c because the new territory has a low density.

These results call for an elaboration of the original equations. Specifically to take into account that for some land uses growth leads to smaller densities. The relaxation factor *R* is introduced which gives the ratio between the density of the pre-existing land and the new area.

$$p^t = \left(\frac{p^{t-1} L^{t-1} + (x-1) L^{t-1} \frac{p^{t-1}}{R}}{x L^{t-1}} \right) x_p = \frac{\left(1 + \frac{x-1}{R}\right) p^{t-1} x_p}{x} \quad (13)$$

Again with:

$$x_p - 1 = E(x-1)$$
$$x_p = 1 + E(x-1) \tag{14}$$

Thus:

$$\begin{aligned} P &= \frac{A}{\left(1+\frac{x-1}{R}\right)p^{t-1}\left(1+E(x-1)\right)L^{t-1}} \\ &= \frac{A}{p^{t-1}L^{t-1}\left(\frac{E}{R}x^2+\left(E+\frac{1}{R}-2\frac{E}{R}\right)x+\left(1-E-\frac{1}{R}+\frac{E}{R}\right)\right)} \end{aligned} \tag{15}$$

Symmetry holds that when land areas reduce in size, the corresponding density grows, meaning that the area that is lost is the area with the lower densities.

For ease the following constants are defined:

$$\begin{aligned} a &= \frac{p^{t-1}L^{t-1}E}{RA} \\ b &= \frac{p^{t-1}L^{t-1}\left(ER+1-2E\right)}{RA} \\ c &= \frac{p^{t-1}L^{t-1}\left(R-ER-1+E\right)}{RA} \end{aligned} \tag{16}$$

The adjusted set of equations can be expressed as follows:

$$F_0(x) = \sum L_i x_i - 1 = 0 \tag{17}$$

$$F_i(x) = a_i x_i^2 + b_i x_i + c_i - a_0 x_0^2 - b_0 x_0 - c_0 = 0 \tag{18}$$

Note that for R = 1 this system simplifies to the original system without the relaxation factor.

This system of equations can be solved numerically, with use of the Jacobean J. Convergence is not guaranteed however and depends on the initial guess for **x**. A reasonable guess is x = 1 for all land uses.

$$J = \begin{bmatrix} L_0 & L_1 & \cdots & L_n \\ -2a_0x_0 - b_0 & 2a_1x_1 + b_1 & \cdots & 0 \\ \vdots & \vdots & \ddots & \vdots \\ -2a_0x_0 - b_0 & 0 & \cdots & 2a_nx_n + b_n \end{bmatrix} \tag{19}$$

4.1.3 Micro level models

At the micro level of Ladamer a model is applied that has been used before in other EU projects (Moland, Murbandy, Medaction) it is the Constrained Cellular Automata (CCA). A characteristic of the CCA is that it uses many parameters, especially for the calculation of the neighbourhood effect. The large amount of parameters may be an obstacle in the calibration process. In order to reduce the complicatedness and to ease calibration the number of parameters in the Ladamer model will be reduced. This is possible by restricting the possible curves of the Neighbourhood Rules. The following sections first describe the Constrained Cellular Automata model consequently the original and adjusted representation of the Neighbourhood rules are discussed. Finally, some preliminary test results are presented.

4.1.3.1 Constrained Cellular Automata

The Constrained Cellular Automata models the detailed allocation of economic activities and people. The model is driven by the demands for land for a region, expressed by acreage for each land use type. The region is represented as a mosaic of grid cells, which together constitute the land use pattern of the region. Four elements determine whether a piece of land (each cell) is taken in by a particular land use function or not.

(1) The physical *suitability*. Suitability is represented in the model by one map per land use function modelled. It is a composite measure, prepared in a Geographical Information System (GIS), on the basis of factor maps determining the physical, ecological and environmental appropriateness of cells to support a land use function and the associated economic or residential activity.

(2) The *zoning* or institutional suitability. Zoning too is characterized by maps, indicating which cells can and can not be taken in by each land use;

(3) The *accessibility*. The accessibility for each land use function is calculated in the model relative to the transportation system. It is an expression of the ease with which an activity can fulfil its needs for transportation and mobility in a particular cell.

(4) *Neighbourhood dynamics.* With neighbourhood dynamics is meant, the impact of land uses in the immediate surrounding of a location. It represents the fact that the presence of complementary or competing activities and desirable or repellent land uses is of great significance for the quality of that location and thus for its appeal to particular activities. For each location, the model assesses the quality of its neighbourhood: a circular area comprising of all cells within a fixed radius. For each land use function, a set of rules determines the degree to which it is attracted to, or repelled by, the other functions present in the neighbourhood. The strength of the interactions as a function of the distance separating the different functions within the neighbourhood is articulated in the *Neighbourhood rules*.

On the basis of these four elements, the model calculates for every simulation step the *transition potential* for each cell and function. In the course of time and until regional demands are satisfied, cells will change to the land use function for which they have the highest potential. Consequently, the transition potentials reflect the pressures exerted on the land.

4.1.3.2 Original representation of Neighbourhood rules

In Moland, Murbandy and Medaction the Neighbourhood Rules are present as distance-weight plots. These distance weight plots are drafted for every pair land uses that is considered relevant. Some land uses are not influenced by Neighbourhood rules, land uses of this type are called *features*.

In a GEONAMICA the Neighbourhood rules are displayed as in Figure 3. Consider here that the blue line graph is really a user interface element, helping the user of the model to set the rule with relatively few mouse clicks. The actual parameters however are found in the table at the right of the dialogue. Now it becomes clear that for every distance found within the neighbourhood a separate parameter is needed. In a neighbourhood with a radius of 8 cell units this accumulates to 30 parameters per rule. The total number of parameters for the land use interaction thus amounts up to

#Parameters = #Features * #Land uses * 30

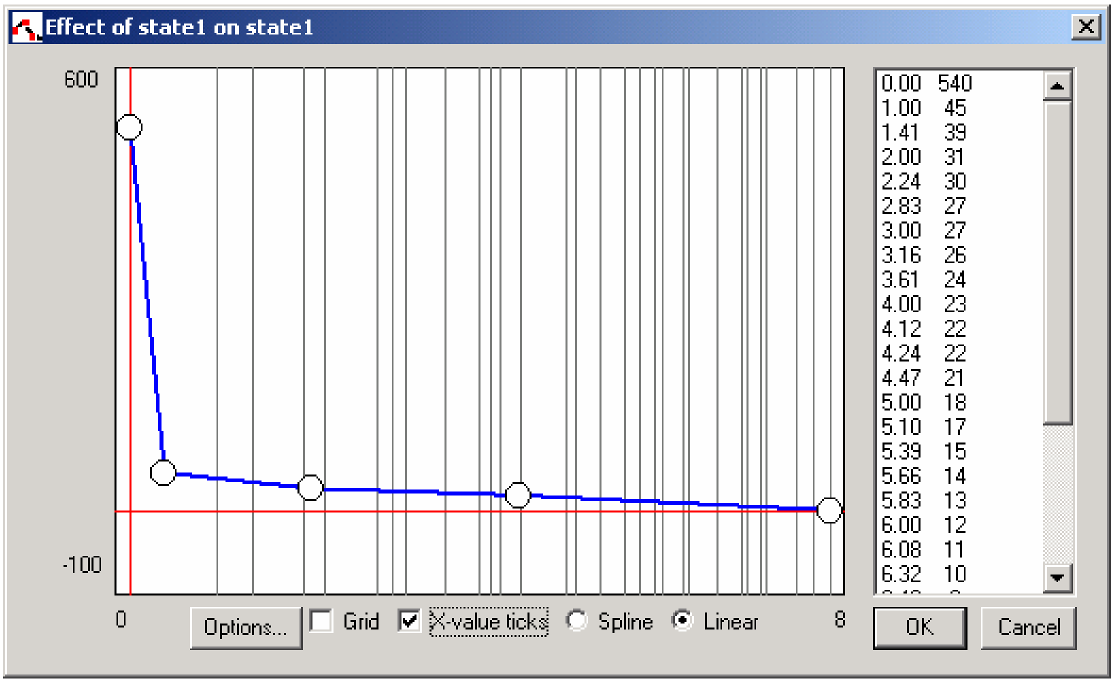

Figure 3: Representation of a neighbourhood rule in the GEONAMICA editor.

With a typical number of 12 land-uses of which 10 are functions this leads to 3600 parameters. This is a lot, but it should be considered that in practice most of these are set to zero, because only relevant land use combinations are included in the model. Furthermore there is a strongly correlated between weights at small distances of each other, and the curves describing the weights at increasing distance seem to be restricted to some archetypical forms. Most typical they are smooth distance decaying functions, although in cases it is found that the influence is negative at small distances and positive at larger distances.

4.1.3.3 Reduced Model

In the reduced version there are still rule sets for all relevant combinations of land uses but instead of a parameters for each distance found in the neighbourhood, the rules are split into rules at zero distance and rules at larger distances. The zero distance rules represent are the values found in the transition matrix.

For distances larger then zero, the neighbourhood rules are to express attraction or repulsion of land uses at distances or a combination of the two. In the CCA with reduced parameter set this is modelled by the combined effect of two exponential distance decay functions. The first part represents the attraction (or pull) of one land use on another; the second is the repulsion (or push) of the same land-use. This functions is given as equation 1.

$$P_{nbh}^{A,B}(d) = \begin{cases} d = 0 : T^{A,B} \\ d > 0 : C_{pull}^{A,B} * e^{\alpha_{pull}^{A,B} * d} - C_{push}^{A,B} * e^{\alpha_{push}^{A,B} * d} \end{cases} \qquad (20)$$

For every pair of land use(A) and feature (B) there are 5 parameters. This means a reduction in the amount of parameters from 30 to 5 = 83% (considering a neighbourhood with an eight cell radius).

#Parameters = #Features * #Land uses * 5

Importantly, the parameters can be explained in terms of transition cost/gain, attraction/repulsion (push/pull) effect and distance decay effects.

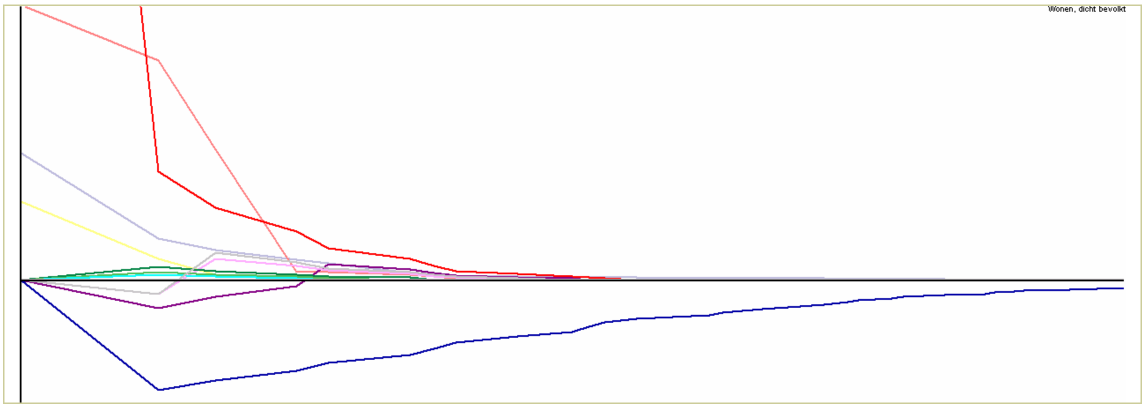

The original manually calibrated rules for the category low density urban area

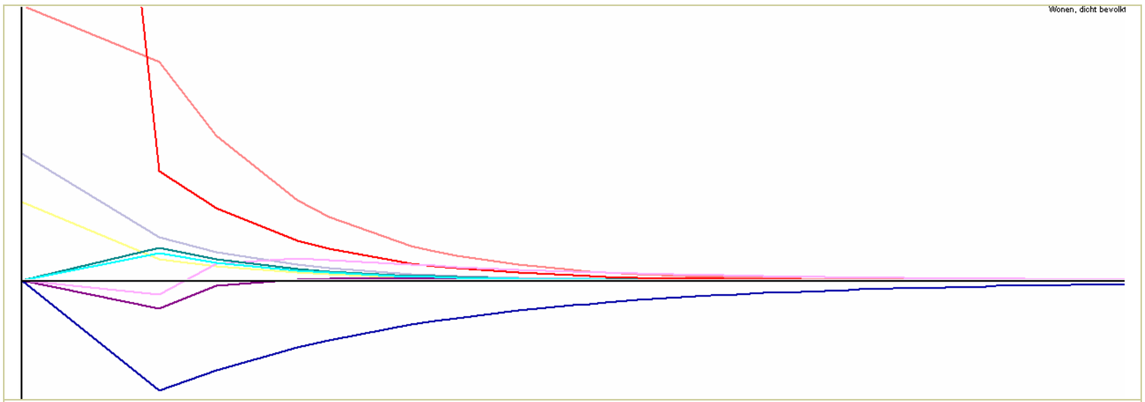

The same curves adjusted to the reduced parameter set

4.1.3.4 Reduced model results

In order to test whether the reduced parameter set negatively influences the model outcomes a test case is considered. The case that is considered is the Moland application for Dublin. A reduced set is constructed by taking the original Moland Neighbourhood rules and fitting them to the exponential function. It would be a possibility to apply a least squared or other fitting procedure for this task. But, considering the idea that it is mainly important that the curves are qualitatively similar and have a similar order of magnitude a procedure is followed in which the parameters are chosen by the modeller directly based upon the original curves whereby the influence at the 1 cell distance is fitted exactly and the distance decay is fitted roughly, consider strong, moderate or weak distance decay.

The model is run with once with the original set of Neighbourhood rules and once with the weights fitted to the exponential curves and it is found that the results are very similar. It is found that the adjusted model produced slightly worse results than the original version. However after some (approx. 1 hour) additional tweaking of the parameters of the exponential curves an even better fit than original was found.

The exponential rule set is calibrated further. This calibration procedure involves running the model for a period in the past (1988-1998), comparing the outcome map with the reality map and adjust the parameters according to the differences that are found.

Map comparison results:

Map 1	Map2	Fuzzy Kappa
Dublin 1998	Dublin 1988	0.90
Dublin 1998	Model 1998 original	0.91
Dublin 1998	Model 1998 fitted curves	0.90
Dublin 1998	Model 1998 fitted curves + extra calibration	0.92

4.2 Area preserving spatial aggregation

The problem: we have maps of a fine spatial scale (either raster or polygon) that we want to use for modelling and analysis on a coarser scale (raster). It is therefore necessary to rescale the original maps.

In a standard rescaling operation where a "majority gets all" procedure is used, often the presence of less prevalent or the more scattered categories will be reduced in this operation.

For the modelling effort it is preferential that the total areas on the map taken in by each category do not depend on the chosen resolution. The rescaling procedure described here aims to preserve the total area taken in by each category at the regional level.

Step 1. Determine number of cells for each category in each region.

The total number of cells in each region is fixed. The number of cells of each category is calculated as the frequency of the category multiplied with the total number of cells.

Since this will in general not give integer outcomes a rounding procedure is necessary.

In first instance all cell totals are rounded down (floor procedure). The remains for each category are remembered (thus the values between 0 and 1) are remembered and the categories are sorted with descending size of the remains.

If the number of cells that still needs to be assigned (thus cells in region – sum of cell for each categories) is *n, t*hen the number of cells for the first *n* categories in the list is incremented by 1.

Step 2. Assigning classes to cells

For each cell the area of each land use is calculated. These areas are *weighted* by multiplying every area with a weightfactor related to the land use class. The reclassed cell will have the category with its highest weighted area. The weights for each class are determined iteratively to satisfy the total number of cells for each category. The initial weight for every category is 1.

The weights are found in the following procedure:

if (demand = 0) then

  $\text{weight}^n = 0$

else if (found = 0) then

  $\text{weigth}^n = (1+\text{Step})*\text{weight}^{n-1}$

else

  $\text{weight}^n = ((\text{demand}/\text{found}-1)*\text{Step} +1)* \text{weight}^{n-1}$

  Where:

  demand = cells required from step 1.

  found = cells found in previous iteration

  weight =weight factor

  Step = MinStep+(MaxStep- MinStep)*2^(-iteration/halftime)

The Step factor decreases with the number of iterations. So that as the procedure progresses higher precision is achieved. The Step-factor initially equals MaxStep, and after *Halftime* iterations it is exactly in between MinStep and MaxStep and finally it will approach MinStep.

The procedure iteratively adjusts the weight factor “less than needed” because the weight factors of other categories are adjusted simultaneaously.

4.2.1 Convergence

Convergence of this algorithm is not guaranteed. Especially in cases where equal area’s are found for many cells. (this is especially the case when rescaling raster maps to other raster maps). In order to obtain better convergence a slight random perturbance is added. This perturbance is added before step 1 when the (unweighted) areas for each category in each cell are determined. This perturbance must have an order of magnitude that is smaller then the smallest contributing area. (cell size of original map, or the smallest intersection of a polygon found in original map, with a cell in the new map).

```
if(area = 0) then
        area adjusted  = 0
else
        area_adjusted = area + random[0, 1]*smallest
```

4.2.2 Complete algorithm

The following is a definition of the algorithm in pseudo-code

```
********************************
**Preparation + random perturbation
********************************

minStep = parameter
maxStep = parameter
maxIterations = parameter
halftime = parameter

cellarea = CalculateAreaOfSingleCell
smallestElement = GetSmallestElement(OriginalMap)
for all cells cel {
        for all categories cat {

                area_in_cell[cel][cat] = AreaOfCategoryCat(cel, OriginalMap)
                if (area_in_cell[cel][cat] != 0) {
                        area_in_cell[cel][cat]  = area_in_cell[cel][cat] + Random(0,1) * smallestElement
                }
        }
}

for all regions r {
        ********************************
        **Step 1
        ********************************
        regioncells = CountNumberOfCells(r, regionmap)

        for all categories c {
                area[c]  = Calculate area of c in r (OriginalMap)
                demand_cells[c] = Floor (area[c] / cellarea)
                rest[c] = Rest (area[c] / cellarea)
        }

        SortedList = AllCategoriesSortedDescendingBy( rest[c] )
        nRest = regioncells - SumAll(demand_cells[c])

        for n = 1 to nRest {
                cat = SortedList[n]
                demand_cells[cat] = demand_cells[cat] + 1
```

```
        }


        *******************************
        **Step 2  -  iteration
        *******************************
        iterationNumber = 0

        for all categories c {
                weight[c] = 1
        }
        iterate = TRUE
        iterationNumber = 0
        while (iterate) {
                for all cells cel in region r{
                        cat[cel] = CategoryWithLargest( area_in_cell[cel][cat] * weight[cat] )
                }

                for all categories c {
                        found_cells[c] = Count(cat[cel] = c)
                        step = minStep +(maxStep- minStep) * 2 ^( - iterationNumber / halftime)

                        if(demand_cells[c] = 0) {
                                weight[c] = 0
                        } else if (found_cells[c] = 0 {
                                weight[c] = weight[c] * (step+1)
                        } else {
                                weight[c] = weight[c] * ((demand_cells[c] / found_cells[c] - 1) * step + 1)
                        }
                }
                success = TestAll(found_cells[c] = demandcells[c])
                cutoff = Test(iterationNumber = maxIterations)
                iterate = NOT (success OR cutoff)
                iterationNumber = iterationNumber + 1
        }
}
```

4.2.3 Spatial aggregation results

The spatial aggregation procedure is applied on a reclassified version of the Corine database. The reclassification is performed according to the scheme presented in Appendix I. The original raster map has a cell size of 250 meter, the map has been aggregated to 1km cells and 8km cells. The illustration below gives an illustration of both results.

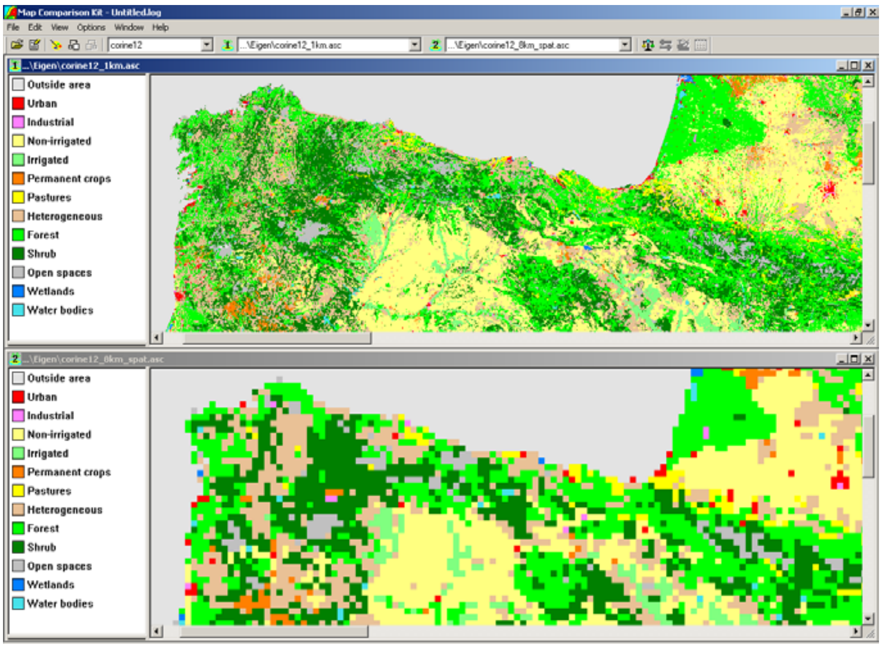

For comparison purposes another 8km aggregation is performed using the Spatial Analyst in ArcMap (ArcView). The illustration below gives both the 1km aggregation by the algorithm described earlier and the 8 km aggregation that is produced by ArcMap.

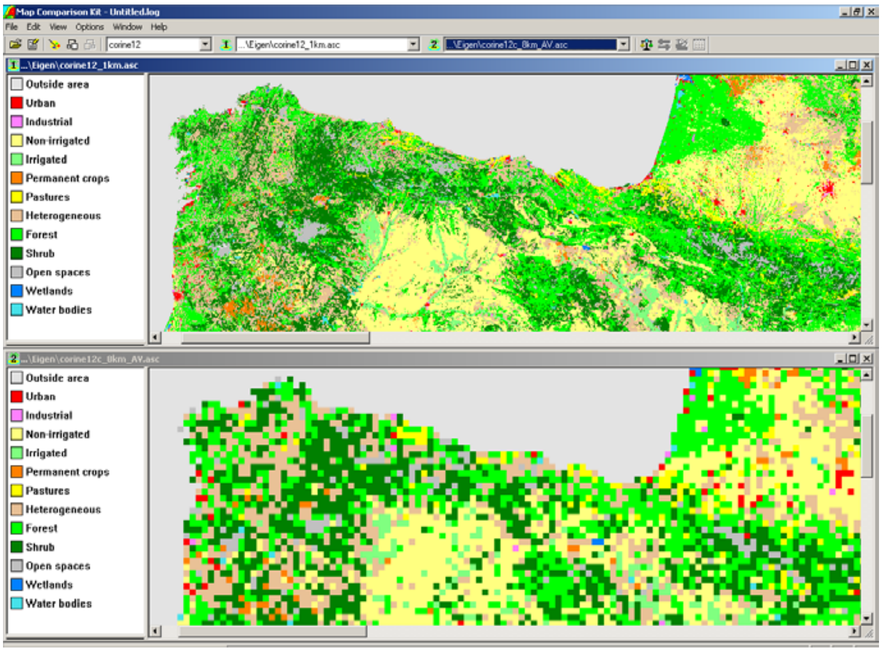

As the illustrations indicate, the aggregation generated by ArcView differs wildly from the one generated by our algorithm. This is unexpected and further research would be necessary to find out what causes the differences. It is also not obvious which algorithm is preferred. It might even depend on the circumstances and the particular application for which the map is needed.

4.3 Calibration and validation

The Ladamer integrated model is intended to be constantly updated given new data from remote sensing interpretations and also other sources. It is major challenge for the land use model to be capable of incorporating this new data, and making the most use out of it. Ideally this means that the model is capable of learning from this new information and will seamlessly adjust its parameters. There are some major problems related to the automatic calibration of the models. These are addressed in the Ladamer project.

Calibration and validation is both a challenge for the macro and the micro level models. The focus so far has been on the micro level models. The reason for this is that the calibration of the micro level model is considered a major concern. One particular area of concern is goodness-of-fit measures for cellular models. In the following section the issue of goodness-of-fit for cellular models is shortly explained. In the remaining two sections two novel methods are introduced.

4.3.1 Goodness-of-fit

The state of the art of evaluation of goodness-of-fit for cellular models involves the cell-by-cell pairwise comparison of model result versus ground truth map and derived statistics. The derived statistics are based upon the correspondence matrix. A reserve against these methods is that they fail to acknowledge two main characteristics of cellular models.

1. Cellular models are spatial. The cell-by-cell pair wise comparison ignores the spatial coherence found in cellular maps. Proximity relations are ignored, as are patterns such as clusters and contiguity
2. Cellular models are dynamic. By comparing result maps with reality it is ignored that cellular models are dynamic, evaluating the models should mean evaluating the dynamic behavior of the model, above comparing the static outcomes of it.

To better evaluate model performance two comparison techniques are developed. The first comparison technique is the Fuzzy Set map comparison assesses map similarity while considering proximity relations and categorical similarity. The second technique is State-Space map comparison. This method aims to compare the nature of transitions that are found in two temporal series of maps.

4.3.2 Fuzzy Set map comparison

The main purpose of the Fuzzy Set map comparison is to take into account that there are grades of similarity between pairs of cell in two maps. The Fuzzy Set approach therefore is fundamentally different from its crisp counterpart, the Cell-by-Cell map comparison, which considers pairs of cells either to be either equal or unequal. The Fuzzy Set approach expresses similarity of each cell in a value between 0 (distinct) and 1 (identical), as the following figure illustrates.

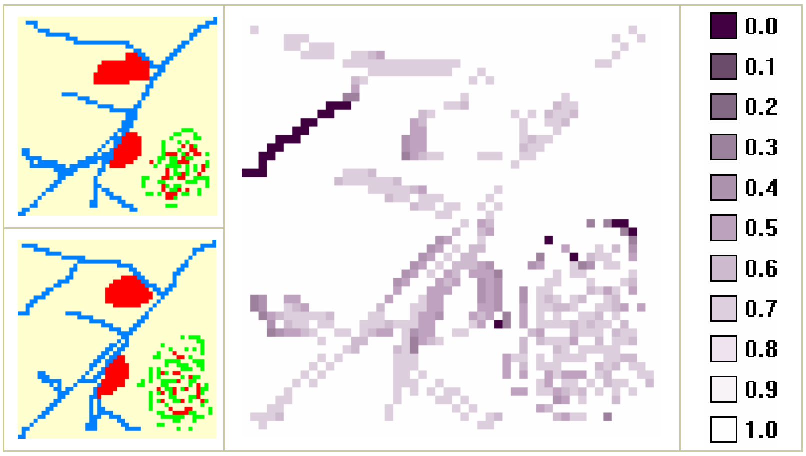

In order to distinguish minor differences from major differences, the Fuzzy Set approach takes two types of fuzziness into account; fuzziness of categories and fuzziness of location.

Besides the result map, also two global similarity indices are calculated. The Average Similarity calculates the average similarity of all cells in the map. A better similarity index is the Fuzzy Kappa, which is the fuzzy equivalent of the Kappa statistic because it corrects average similarity for the similarity to be expected given the fractions of land taken in by each category.

4.3.2.1 Fuzziness of Location

In a categorical map (e.g. a land use map) each cell is taken in by a certain category. In reality this does seldom mean that the area of the cell is solely taken in by that particular category. In many cases it means that this category is known or expected to be present in that neighbourhood and that the cell is mostly in accordance with that category. This fuzziness of location is taken into account, by letting the fuzzy representation of a cell be partly defined by the cells found in its proximity. The level to which neighbouring cells influence a cell is set with a function. Three types of functions have been implemented *Exponential decay*, *Linear decay* and *Constant value*. Each of these functions takes a parameter, respectively: *Halving distance*, *Slope* and (constant) *Value*. It is in principle possible to apply two different functions for the two maps, for the time being however it seems that interpretation of comparisons based on a single function is already complicated enough.

4.3.2.2 Fuzziness of categories

The definition of categories in maps is often imprecise. This is especially true if some or all categories on the map have in fact an ordinal definition, such as for instance the categories ‘high-‘, ‘medium-‘and ‘low-density residential area’ on a land use map. The boundaries between such categories are less clear-cut than what seems to be the case from the legend. This is called fuzziness of categories. In order to take fuzziness of categories into account when comparing maps it is necessary to fill out the *Category Similarity* Matrix. In the matrix the similarity between each pair of categories from the legend is specified with a number between 0 (crisply distinct) and 1 (completely identical). By default the categories are set to be crisply defined, which means that the category matrix is set to unity.

4.3.3 State-Space map comparison

A novel method specifically aimed at the comparison of spatial dynamics, that is transitions or changes in maps, is the state-space map comparison. The main idea is to capture the dynamics that are found in series of maps (minimally a "before" and an "after" map) by considering the number of transitions that are found from one location in "State-Space" to another.

The method is new, but use of State-Space models is common in chaos theory and complexity modelling. A similar approach has been applied before for the evaluation of braided rivers models (by Murray & Paola).

A state-space is a set of characteristics of a location that are relevant to the dynamics of the system. Sites change from one location in state-space to the next location in state-space. The state-space comparison compares the transitions in state-space that are found in two sets of "before" and "after" maps.

For the state space comparison the state space is made discreet (thus state space is a multidimensional grid, consisting of multidimensional cells). The comparison result is made up by the total difference of percentage of transitions per cell of origin in state-space.

4.3.3.1 Traffic light example

The following is a simple example of the state-space comparison of two types of traffic light. A traffic light only has three distinct states (locations in state space), being: green, yellow and red.

Two traffic light regimes are considered the first works according to the following time loop

Light loop 1:
Green 60 seconds
Yellow 20 seconds
Red 60 seconds

The second has the following regime

Light loop 2:

Green 40 seconds
Yellow 15 seconds
Red 40 seconds
Yellow 15 seconds

When the traffic light are observed very often, everytime with ten-second interval between the "before" and "after" observation, then the following transition matrices will be found.

t+10s

t		83%	17%	0%
		0%	50%	50%
		17%	0%	83%

Loop 1.

t+10s

t		75%	25%	0%
		33%	33%	33%
		0%	25%	75%

Loop 2.

t+10s

t		8%	8%	0%
		33%	17%	17%
		17%	25%	8%

Difference (total = 133)

The total difference of percentages that thus is found is the resulting difference of the state space comparison.

In a regular state space comparison there are much more then 3 possible states. A comparison considering three different characteristics, each discrete in 20 intervals will have 20^3=8000 possible states. For the comparison of before and after maps, there are not a lot of observations at different moments in time, instead there are many observation at different locations in (geographical) space.

4.3.3.2 State-space test case

The state-space comparison is tested on the Moland model of Dublin. The dimensions of state space are made up by the presence of 5 main land use types in the neighbourhood of a cell. These land use types are:

- Nature
- Agriculture
- Residential
- Commercial
- Industrial

The presence is measured as a percentage of cell within a four cell radius and made discrete with 10% intervals. Each cell on the map belong to one of 10^5 possible states.

Four sets of before and after maps were compared and the comparison results are in line with what is expected from expert judgment. The four sets are:

Set 1: Dublin 1988 – Dublin 1998

Set 2a: Dublin 1988 – Dublin Model 1998 (First Calibration)

Set 2b: Dublin 1988 – Dublin Model 1998 (Improved Calibration)

Set 2c: Dublin 1988 – Dublin 1988

As expected the difference between Set 1 and Set 2a is slighty larger than the difference between Set 1 and Set 2b but a lot smaller then the difference between Set 1 and Set 2c.

4.3.3.3 Outlooks on state-space comparison

The main advantage of the state space comparison is that it considers spatial dynamics instead of static model results. Another advantage is that it is a template-free comparison. Whereas most comparison method can only compare maps of the same area this is not required for the space state comparison. Thus it becomes possible to compare for instance the spatial development of southern Italy with that of Portugal. Because of this characteristic the state-space comparison may also be used to identify different types of spatial behaviour.

There is still work to be done on the algorithm as well though. The summation of differences in fractions is quite a crude method and alternative approaches may be found in the literature. Also the current implementation offers a black box comparison, it gives a measure for the difference between two pairs of maps. The calibration and validation process of cellular models will better supported if the method can give more insight in the nature of the differences.

Appendix I: Reclassification scheme for Corine LC map

Urban	1.1 urban fabric 1.1.1 Continuous urban fabric 1.1.2 Discontinuous urban fabric 1.4 Artificial non-agricultural vegetated areas 1.4.1 Green urban areas 1.4.2 Sport and leisure facilities
Industrial	1.2 Industrial, commercial and transport units 1.2.1 Industrial or commercial units 1.2.2 Road and rail networks and associate land 1.2.3 Port areas 1.2.4 Airports 1.3 Mine, dump and construction sites 1.3.1 Mineral extraction sites 1.3.2 Dump sites 1.3.3 Construction sites
Non-irrigated Arable	2.1 Arable land 2.1.1 Non-irrigated arable land
Irrigated Arable	2.1.2 Permanently irrigated land 2.1.3 Rice fields
Permanent	2.2 Permanent crops 2.2.1 Vineyards 2.2.2 Fruit trees and berry plantations 2.2.3 Olive groves
Pastures	2.3 Pastures 2.3.1 Pastures
Heterogeneous	2.4 Heterogeneous agricultural areas 2.4.1 Annual crops associated with permanent crops 2.4.2 Complex cultivation patterns 2.4.3 Land principally occupied by agriculture with significant areas of natural vegetation 2.4.4 Agro-forestry areas
Forests	3.1 Forests 3.1.1 Broad-leaved forest 3.1.2 Coniferous forest 3.1.3 Mixed forest
Shrubs	3.2 Shrub and/or herbaceous vegetation associations 3.2.1 Natural grassland 3.2.2 Moors and heathland 3.2.3 Sclerophyllous vegetation 3.2.4 Transitional woodland/shrub
Open spaces	3.3 Open spaces with little or no vegetation 3.3.1 Beaches, dunes, sands 3.3.2 Bare rock 3.3.3 Sparsely vegetated areas 3.3.4 Burnt areas 3.3.5 Glaciers and perpetual snow
Wetlands	4.1 Inland wetlands 4.1.1 Inland marshes 4.1.2 Peatbogs 4.2 Coastal wetlands 4.2.1 Salt marshes 4.2.2 Salines 4.2.3 Intertidal flats
Water bodies	5.1 Inland waters 5.1.1 Water courses 5.1.2 Water bodies 5.2 Marine waters 5.2.1 Coastal lagoons 5.2.2 Estuaries 5.2.3 Sea and ocean

WP 5 – Validation and methodological refinements

5.1 Main work carried out during the reporting period (summary)

During the reporting period JRC contributed to the collection of relevant regional scale data layers (WP 2.1), to the establishment of methodology to derive of vegetation cover density from NOAA-AVHRR data (WP 2.2). Main focus was on the review of existing regional scale assessments of Mediterranean land degradation, in order to assess options for LADAMER product evaluation, validation and quality assessment (WP 5).

5.2 Main achievements

5.2.1 Contribution to WP2.1: Building of a spatial data base

Main focus was to contribute to the collection of regional scale remote sensing data, meteorological data and Europe-wide thematic data layers produced by EUROSTAT-GISCO.

The following data sets have been obtained and delivered for use in the thematic work packages 2 and 3, respectively for integration in the LADAMER spatial data base:

- MARS NOAA-AVHRR archive
- MARS gridded meteorological data
- GISCO spatial data layers

All 3 types of data are considered core input to the LADAMER approach to regional land degradation assessment. Although all data sets are produced for operational use of Commission activities, it has to be reviewed to what extend they currently meet the needs of LADAMER and more general of GMES in terms of spatial/temporal coverage, availability/accessibility and of data quality.

MARS NOAA-AVHRR archive:

The archive has been created and is managed by the MARS project (Monitoring Agriculture by Remote Sensing), run by the JRC Institute for Protection and Security of the Citizen (JRC-IPSC, MARS Unit). MARS is operationally using the data for the retrieval of Europe wide NDVI profiles of various crop types and of thermal information for monitoring and assessing crop development during the growing season and in the context of crop growth forecasting.

Spatial/temporal coverage:

The archive covers a time period from 1989 to 2002 and is continuously up-dated. It contains daily 1 km NOAA-AVHRR data and derived products such as 10 days maximum value composites of NDVI and surface temperature (Ts), re-sampled to 4x4km pixels. It covers entire Europe, Turkey and NW-Africa (Mediterranean parts, see Fig. 1).

The spatial and temporal coverage and resolution is in principle suitable for LADAMER.

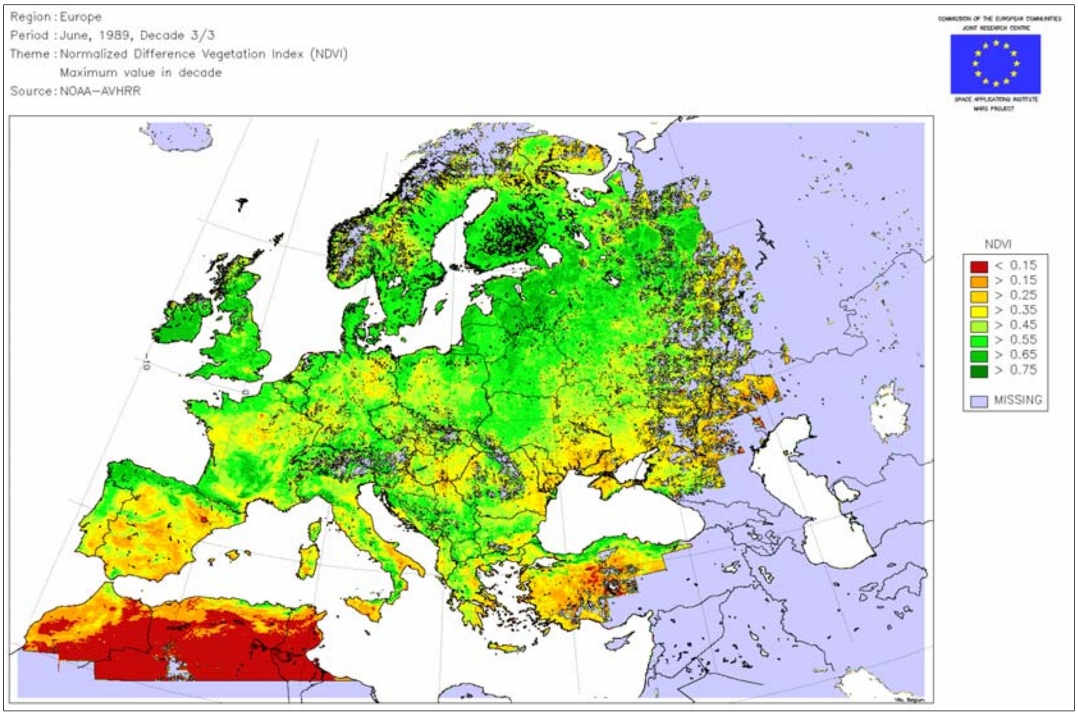

Figure 1: Spatial coverage of MARS NOAA-AVHRR archive (NDVI 10 days composite)

Data availability/accessibility:

The data set is available upon request to be used in research projects and for other purposes of the European Commission.

The archive is structured in 5 levels of data processing products ranging from raw data of AVHRR spectral channels to derived daily NDVI and Ts channels at 1 and 4 km sampling and 10 days composites of NDVI and Ts at 1 and 4 km sampling. The overall data base (all levels of data and derived products) amount to

In its main parts the archive is stored on optical media (CD/DVD) and can not be made accessible on-line. Only level 4 and 5 data are currently held in on-line storage but can not be directly accessed from outside the JRC.

The MARS project granted full access to the data base for the purposes of LADAMER, but has no resources to provide data access and distribution services. Indeed, given the large quantity of data (2.645 Tbyte), just the copying of the archive required a considerable amount of resources in terms of man-power, IT infrastructure for archive reading, intermediate storage and CD/DVD production and purchase of storage media. Set-up of infrastructure and the archive reproduction was implemented by partner 4 at the JRC with man-power support from partner 1, detaching 1 member of staff for a couple of weeks to the JRC.

Nevertheless the effort appears to be justified, since the data set constitutes the only 1 km archive that is available in its entirety to the project. Similar data sets such as MEDOKADS or USGS pathfinder, which are also evaluated in the project, have limitations in spatial resolution and length of time series (e.g pathfinder full time series available only 8x8km, 1 km only 3 years), or in the accessible coverage (e.g MEDOKADS, presently only Spain).

Data quality:

The MARS unit has established a standardised processing chain for radiometric calibration and atmospheric correction based on standard atmospheric parameters and state-of-the-art algorithms. In subsequent steps geometric correction and 10 days mosaicking is performed. The system has recently been re-shaped under the name SpacePC+ (VITO 2002) and the full archive has been re-processed, mainly to overcome a number of drawbacks of radiometric pre-processing. While clear improvements of radiometric data quality could be achieved, the archive suffers from substantial problems of geo-metric co-registration (stacking) of the images of different observation dates. These errors in spatial co-registration are a major source of noise in the data. In addition the time series suffer from a number of substantial data gaps especially in the winter months. Nevertheless the problems are well documented, the data structure and processing chain are fully documented and transparent (VITO 2002).

JRC has investigated a number of options to improve the accuracy of scene to scene co-registration and to close temporal data gaps by advanced interpolation algorithms. These may be valid options to generate in phase 2 a more complete spatial and temporal coverage of 1 km data over the entire LADAMER project area, in case other sources (e.g. MEDOKADS) may not be accessible for the whole Mediterranean.

MARS re-gridded meteorological data

Meteorological data are a core input to WP 3on Land Degradation Modelling and Assessment.

Spatial/temporal coverage:

This data set has been derived from the original 50x50 km grid daily weather data archive produced by the MARS project for the Crop Growth Monitoring System (CGMS, http://mars.jrc.it/stats/cgms/) covering the whole of Europe with daily records over more than 20 years.

The original data set provides interpolated (50x50 km grid) daily maps of:

Value	Description
MAXIMUM_TEMPERATURE	maximum temperature (°C)
MINIMUM_TEMPERATURE	minimum temperature (°C)
VAPOUR_PRESSURE	mean daily vapour pressure (hPa)
WINDSPEED	mean daily windspeed at 10m (m/s)
RAINFALL	mean daily rainfall (mm)
E0	Penman potential evaporation from a free water surface (mm/day)
ES0	Penman potential evaporation from a moist bare soil surface (mm/day)
ET0	Penman potential transpiration from a crop canopy (mm/day)
CALCULATED_RADIATION	daily global radiation in $KJ/m^2/day$

Table 1: Available gridded data in MARS meteo data base:
http://mars.jrc.it/documents/stats/cgms/GridWeather.pdf

Data availability/accessibility:

MARS can only make available these derived products but not the data of the approximately 1400 meteo stations across Europe being used for their generation, due to copyright restrictions.

These 50x50 km data have been re-gridded to 1km cell size applying additional weighting factors to better account for factors like distance to coast and altitude. This work was originally performed to suite the needs of the EU funded PESERA project (Pan European Soil Erosion Risk Assessment) aiming at developing and validating a standardised physically based model of erosion risk assessment at pan-European level and 1 km resolution.

Approval to freely use the data in LADAMER has been obtained both from the MARS project and from the PESERA consortium (http://pesera.jrc.it/).

Data quality:

The data set suffers from a number of inconsistencies in the input data and the original interpolation procedure, as well as from the relatively small number and uneven geographical distribution of stations. However it has to be mentioned that it is currently the only record of daily meteorological data for the whole of Europe, which is freely available.

GISCO spatial data layers

GISCO data sets are primarily required for WP 4 on land use change modelling and have been made available through the data server of the IES Land Management Unit. The JRC receives the regular up-dates of the entire spatial data base released by GISCO and provides access to all meta-data through their web site.

general metadata: http://data-dist.jrc.it/en/data-dist/

gisco: http://data-dist.jrc.it/eu4u/metadata/index.html?plain

The following data sets have been made available free of charge through this channel, upon the basis that JRC is project partner in LADAMER.

Theme AD = Administrative data
- Layers NU* = NUTS regions

Theme HY = hydrography
- Layer WS* = watersheds
- Layer WP* = waterpattern

Theme IN = infrastructure
- Layer AP* = airports
- Layer PO* = ports
- Layer FL* = ferry links
- Layer RD* = roads
- Layer RW* = railways
- Layer ST* = settlements

Theme EN = environent
- Layer SE = soil erosion
- Layer LQ = land quality

Theme LR = land resources

Layer LC = land cover
Layer SL = soils
Theme NR = nature resources
Layer BG = biogeographical
Layer BP = biotopes
Layer DA* = designated areas
Layer VG = natural vegetation
Layer LS = landscapes

Data availability/accessibility:

GISCO data are in principal freely available and accessible via the GISCO data stores. However, GISCO distributes the data on CD and although GISCO does have no commercial interest, they charge a fee as compensation for the base cost of data reproduction and distribution, which can reach a considerable amount beyond a symbolic cost. The delay of data delivery (several months) that was announced by GISCO turned out to be a greater problem than the cost and could have let to a critical delay in WP 4, if the regular GISCO channel would have been the only option. Direct data delivery to LADAMER by JRC was only justified on grounds of JRC participation in the projects.

Data extraction from the overall data base and direct transfer via ftp was very straight forward and worked without any problem or delay.

5.2.2 Contribution to WP2.2: Geoinformatics and remote sensing analysis

In close collaboration with partner 1 options to derive vegetation density maps at 1 km resolution for the entire LADAMER test area have been evaluated. It is proposed to implement and evaluate an approach, which uses the feature space of NOAA-AVHRR NDVI and Ts channels in a spectral mixture model.

Although it is known, that both NDVI and Ts are varying not exclusively as a function of vegetation cover, linear approximations to explain NDVI and Ts of mixed (vegetation/non-vegetation) AVHRR pixels in relation to vegetation have been given:

According to Price (1989) the NDVI of a mixed pixel can be written as

$$\mathbf{NDVIp = (f)NDVIv + (1\text{-}f)NDVIn}$$

where v and n indicate vegetation and non-vegetation and f the proportional fraction of vegetation in the pixel.
Equally Caselles & Sobrino (1989) give for Ts of a mixed pixel

$$\mathbf{Tp = Pv{*}Tv + (1\text{-}Pv)Tn}$$

where Tp is the pixel temperature, v and n indicate vegetation and non-vegetation and Pv is the proportion of vegetation in the pixel

Of course these simplified, linear equations do not account for effects such as internal reflections or shading, nevertheless these approximations have been repeatedly empirically confirmed in NDVI/Ts regression models applied to AVHRR data of areas with variable vegetation cover (Lacaze et al., 1996; Nemani et al., 1993). Although NDVI as well as Ts have been observed to be variable also in dependence of the vegetation type, it is of utmost importance for our approach that under dry conditions the slope of the vegetation/non-vegetation line proved to be very stable. Nemani et al. (1993) observed for a wide range of North American grassland, forest and crops the same NDVI/Ts relation (i.e. the same slope), which was considerably changing only under wet surface conditions or in presence of strong climate gradients (e.g. in mountainous regions). The same can be observed in the scattergrams of monthly NDVI/Ts averaged over several years at a Mediterranean wide coverage.

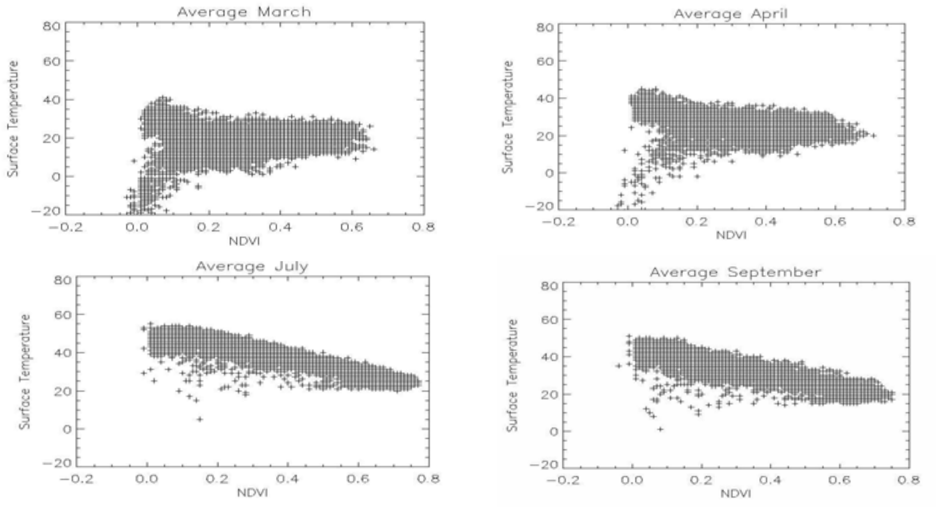

Figure 2: Monthly averages of NDVI-Ts relationship for the entire Mediterranean region derived from 13 years of 8 km resolution data.

In figure 2 we notice the difference between March/April and July/September. The dry summer months exhibit a stable linear arrangement of all pixels along he NDVI-Ts line between the co-ordinates of bare surfaces (upper-left) and densest vegetation cover (lower right). In the 2 spring examples, this distribution is distorted, mainly along the temperature axis, due to the highly increased presence of clouds and snow expressing also the climatic gradient in the region not being evident in the 2 presented summer months.

Against this background we conclude that under dry conditions the position of a mixed AVHRR pixel in relation to NDVI and Ts co-ordinates should be primarily controlled by fractional vegetation cover, being approximately scaled in a linear way by the extremes of non-vegetated and completely vegetation covered pixels. Thus it should be possible to estimate directly fractional vegetation cover from this relationship if we are able to determine the co-ordinates of the extremes and to control the influence of temperature variability due to soil moisture, abundant water, snow, clouds or along strong climatic gradients (e.g. at high mountains).

Linear unmixing and related techniques provide a number of possibilities, which appear particularly well suited to solve these problem as it is equivalent to the determination of endmembers.

This approach has been already defined within the Demon and MEDALUS projects and tested on limited 1 km data sets and the entire pathfinder 8 km time series of the entire

Mediterranean. The results of these test indicate that the derived vegetation abundance time series is less affected by effects of sensor drift that can be observed if vegetation trends are analysed on the basis of the NDVI alone ("greening of deserts" and increase of NDVI on evergreen dense vegetation).

These 8km time series of NDVI-Ts unmixing derived vegetation abundance or green vegetation fraction (GVF) have also been used as input to estimate annual NPP expressed as the mean of monthly values of the GVF, which was then further used for the calculation of regional trends of changes in rain use efficiency (RUE) as degradation indicator. Especially the estimates of sparse vegetation seem to be improved in comparison to the pure NDVI approach (Lacaze et al., 2003).

Further testing of the approach on the available MEDOKADS data is underway.

5.2.3 Work Package 5: Validation and methodological refinement

Given the small scale respectively the coarse resolution (1 km2 grid cells) of the LADAMER products, a field validation of LADAMER results will be hardly feasible. The proposed alternative is to evaluate the quality or rather the plausibility of the model outputs of WP3/WP4 against the results of previous regional scale land degradation studies that have been undertaken in the Mediterranean Basin as part of research programmes or of long term early warning system.

In a first step, a review of existing regional scale assessments of Mediterranean land degradation has been undertaken. A review of the most relevant projects and assessments, that operate on the LADAMER area of interest and that have produced data sets suitable for comparison are listed in table 2.

Following the collection of detailed information about the data and products used and produced by these projects, now a detailed evaluation of the conceptual models that were used to asses the state of desertification or the sensitivity to desertification threats is underway in order to allow meaningful comparisons between different products and method and the products of the first phase of LADAMER.

Name	Major objective	Type of data	Location / scope
Long Term Early Warning Systems			
Long Term Ecological Monitoring Observatories Network (**ROSELT**)	Monitoring aimed at desertification assessment	Vegetation changes in relation to social and technical changes.	Circum sahara (Regional)
The Global Assessment of Human Induced Soil Degradation (**GLASOD**)	Mapping of land degradation	The GLASOD database contains information on soil degradation within map units as reported by numerous soil experts around the world through a questionnaire. It includes the type, degree, extent, cause and rate of soil degradation. From these data, GRID produced digital and hardcopy maps and made area calculations.	Global
Land Use and Cover Change (**LUCC**)	To monitor and model land use and cover change	Databases on: socio-economic driving forces associated with geo-referenced land use and land cover changes. Geo-referenced integrated land use and land cover data providing accurate information on their rates of change of use. Data for describing and characterising global-scale processes in the land surface and their interactions with global biogeochemical cycles and climate.	Global
Research Projects			
Remote sensing on Mediterranean desertification and environmental stability; RESMEDES / RESYSMED	Defining indicators for desertification neasurements by RS	- European and Mediterranean NDVI/albedo time series (with cloud cover) 1995-1997 and reconstructed cloud free time series - iso-growth zones map based upon Fourier components - relationship between NDVI and precipitation/net radiation, necessary to detect and classify climate sensitive areas - SEBI method to calculate energy balance parameters from satellite images - HANTS algorithm to perform an error- and cloud free Fourier analysis	Europe (Regional)
Mediterranean Desertification and Land Use (**MEDALUS**)	The interactions of land use changes on desertification	soils, land use, vegetation, climate and hydrology	Med. Europe (Regional)
DEMON and GeoRange	Land Degradation Induced by disturbance (e.g. fire, grazing pressure)	Landsat images (large set), field spectrometry, lithology, access roads, morphological parameters	Med. Europe (regional)
PESERA	Pan European Soil Erosion Asessments	Regional scale soil information system, meteorological data, soil erosion risk scenarios at 1 km resolution	Europe
DesertLinks	Development of desertification indicator system for the Mediterranean Basin	Regional and local maps of desertification indicators, environmentally sensitive areas (ESAs), data base of desertification indicators	Medit. Europe
Medaction	Develop integrated policy options and mitigation strategies to combat desertification	Mediterranean and local land use change scenarios,	Medit. Europe

	in the Northern Mediterranean		
DISMED	Creation of common information system to monitor the physical and socio-economic conditions in areas threatened or affected by desertification	National and regional desertification sensitivity maps, based on vegetation trends, land use/cover information,	Entire Medit. Basin
CAMELEO	to develop methodologies for the identification of remotely sensed indicators of desertification	Data and information inventory, local ecological change detection, change assessment in the regional and global context, human dimension of the changes, analysis and interpretation of the changes.	Med. Africa (Regional)

References

Lacaze B., Ait-Bachir S. and Sommer S., 2003: Analyse diachrinique de l''efficacite des pluies pour la production vegetale dans le bassin mediterraneen de1982 a 1996. *Télédétectio*n, 2003, vol. 3, n° 2-3-4, p. 285–294

Lacaze B., Caselles C., Coll C., Hill J., Hoff S., de Jong S., Mehl W., Negendank J., Riezebos H., Rubio E., Sommer S., Teixeira Filho J. & Valor E., 1996: DeMon Integrated Approaches to Desertification Mapping and Monitoring in the Mediterranean Basin. Final Report of the DeMon-1 project. EUR 16448 EN, JRC Ispra, 176pp.

Nemani P., Pierce L., Running S.W. & Goward S., 1993: Developing satellite derived estimates of surface moisture status, Journal of Applied Meteorology, Vol., 32, 548-557.

Price, J.C., 1993, Estimating leaf area index from satellite data, *IEEE Transactions on Geoscience and Remote Sensing*, vol. 31, no. 3, 727-734.

http://www.icis.unimaas.nl/medaction/

http://www.kcl.ac.uk/kis/schools/hums/geog/desertlinks/index.htm

http://dismed.eionet.eu.int/#

WP6 – Dissemination and end-user integration

6.1 Lessons learned

On Work Package 6 we are still at an early stage, as LADAMER final product is being developed. It is one first difficulty we have faced, to find end-users and assess their interest and ability to manage a product not yet created.

Another difficulty has been arising at launching the enquiries on large EU and Global stakeholders, as at this level it is difficult to directly reach someone who can answer on behalf of the institution, and simultaneously give us his personal view on LADAMER products. Using e-mail communication is a simplifying tool, but it does not assure a timing response.

Another relative difficulty is related to the Policies dynamics and the changing role of institutions in what concerns Land Degradation. The current implementation of the EU Soil Thematic Strategy is a good example of such changes, which are not always easy to follow and update.

6.2 Information products

A major task developed at this early stage of LADAMER Project was to identify the main stakeholders on Land Degradation Management and Assessment, both at the National, EU and Global levels. This provided a wide **list** of potential end-users of LADAMER products, which are now being integrated into **schemes**, providing information on their functions and hierarchic relationships.

Secondly, a simple and preliminary **enquiry** is being set forward and launched to all the previously identified institutions, in order to assess these end-users needs and involvement concerning land degradation management and assessment. More specifically, it will enquire on their interest and ability to use a cartographic model for Land Degradation management.

The results will be integrated into a **database** which will provide us an overview of end-users interests and needs. Based on these results, a **second enquiry** will be launched on specific requirements and knowledge needed to use LADAMER products, as well as on its potential results. This second enquiry will be more detailed and specifically targeted at core institutions.

Appendix I: List of potential end-users in Portugal

End-users definition

In Portugal, the use of modelling tools for land use planning and management is strongly concentrated on governmental organisations, at the national (A) and regional level (B).

Other institutions potentially interested in the use of such models include the larger environmental NGO's (C), and also some enterprises working on environmental planning (D).

A – National GO's

SNPC – Serviço Nacional de Protecção Civil (MAI)
Av. do Forte – Lisboa
214 247 100

DGF – Direcção-Geral de Florestas (MADRP)
Av. João Crisóstomo, 28 – Lisboa
213 124 800

IFADAP – Instituto de Financiamento e Apoio ao Desenvolvimento da Agricultura e das Pescas (MADRP)
Av. João Crisóstomo, 11 – Lisboa
213 116 200

IHERA – Instituto de Hidráulica, Engenharia Rural e Ambiente (MADRP)
Av. Afonso Costa, 3 - Lisboa
218 442 200

INIA – Instituto Nacional de Investigação Agrária (MADRP)
Rua Barata Salgueiro, 37, 4º - Lisboa
213 131 700

DGA – Direcção-Geral do Ambiente (MCOTA)
Murgueira – Carnaxide
214 728 200

ICN – Instituto de Conservação da Natureza (MCOTA)
Rua da Lapa, 73 – Lisboa
213 938 900

IGA – Inspecção-Geral do Ambiente (MCOTA)
Murgueira – Carnaxide
214 728 324

IGP – Instituto Geográfico Português (MCOTA)
Rua da Artilharia Um, 107 – Lisboa
213 819 600

IOA – Intervenção Operacional de Ambiente (MCOTA)
Rua do Século, 51, 2º - Lisboa
213 231 610

INAG – Instituto da Água (MCOTA)
Av. Almirante Gago Coutinho, 30 – Lisboa
218 430 000

IGeoE - Instituto Geográfico do Exército (MD)
Av. Dr. Alfredo Bensaúde – Lisboa
218 505 300
http://www.igeoe.pt

B – Regional GO's

CCRN – Comissão de Coordenação da Região Norte
Porto

CCRC – Comissão de Coordenação da Região Centro
Coimbra

CCRLVT – Comissão de Coordenação da Região de Lisboa e Vale do Tejo
Rua da Artilharia Um, 33 – Lisboa
213 812 073

CCRA – Comissão de Coordenação da Região Alentejo
Estrada das Piscinas, 193 – 7000 Évora
266 740 300

CCRAL – Comissão de Coordenação da Região Algarve
Faro
Governo da Região Autónoma dos Açores
Ponta Delgada

Governo da Região Autónoma da Madeira
Funchal

C – Environmental NGO's

LPN – Liga para a Protecção da Natureza
Estrada do Calhariz de Benfica, 187 – Lisboa
217 780 097

QUERCUS-ANCN – Associação Nacional de Conservação da Natureza
Calhau – Lisboa
217 788 474

GEOTA – Grupo de Estudos de Ordenamento do Território e Ambiente
Travessa do Moinho de Vento à Lapa, 17, cv.D – Lisboa
213 956 120

D – Private Enterprises

FBO-Consultores SA
Rua Dr. António Leitão Borges, 5, 6º - Miraflores – 1495-131 Algés
214 127 400
http://www.fbo.pt

NEMUS – Gestão e Requalificação Ambiental Lda.
Estrada do Paço do Lumiar, Edifício R, 2º, sala 203 – Lisboa
217 110 946

HIDROPROJECTO – Engenharia e Gestão SA.
Av. Marechal Craveiro Lopes, 6 – Lisboa
217 513 000

HIDRORUMO

PROENGEL – Projectos, Engenharia e Arquitectura Lda.
Rua Manuel R. Silva, 7-C, sala 4 – Lisboa
217 121 080

ERENA – Ordenamento e Gestão de Recursos Naturais Lda.
Av. Visconde Valmor, 11, 3º - Lisboa
217 991 100

Appendix II: End-users' schemes

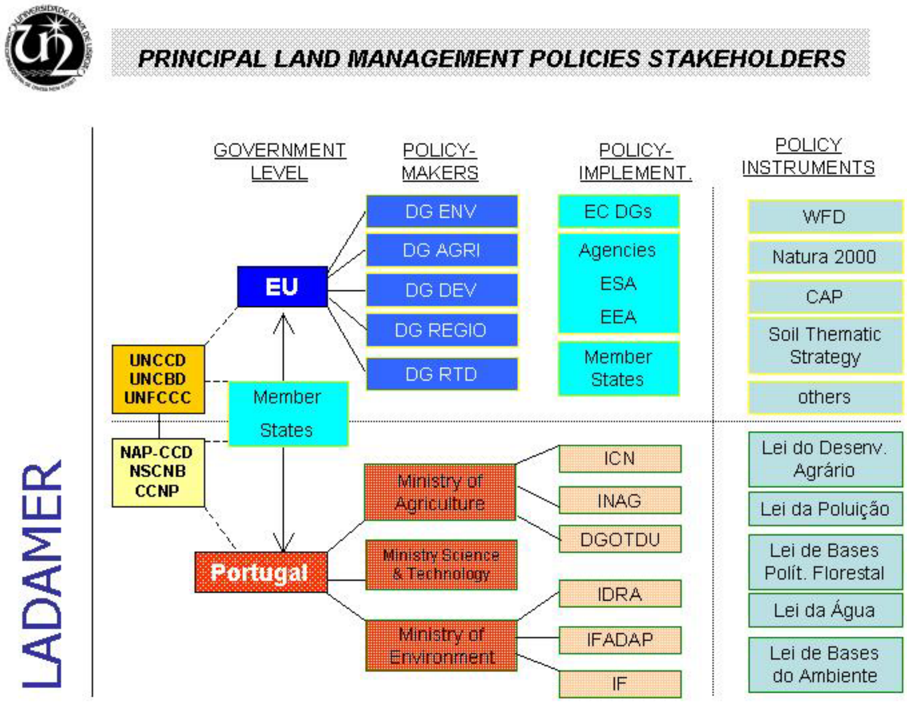

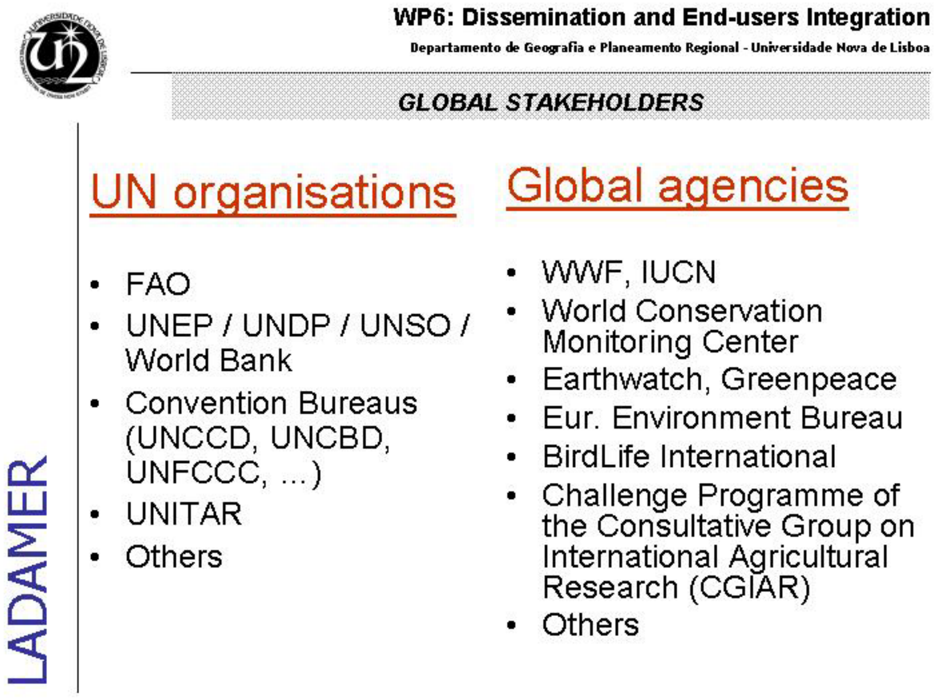

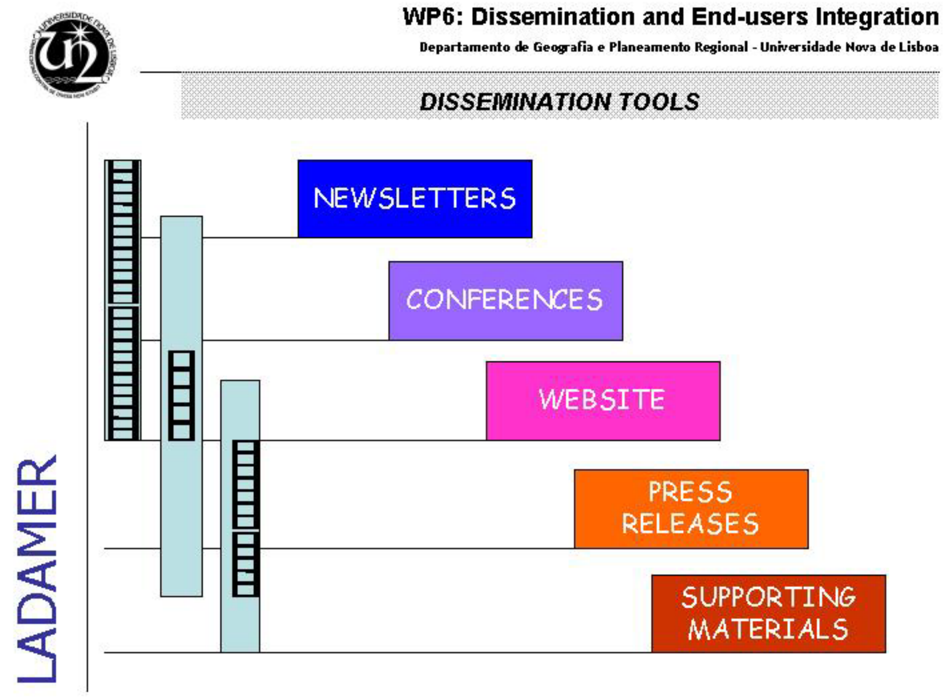
WP6: Dissemination and End-users Integration
Departamento de Geografia e Planeamento Regional - Universidade Nova de Lisboa
DISSEMINATION TOOLS
LADAMER
NEWSLETTERS
CONFERENCES
WEBSITE
PRESS RELEASES
SUPPORTING MATERIALS

Appendix III: LADAMER enquiry on end-users' needs

1. Institution name ______________________________

2. Type ______________________________

3. Address ______________________________

4. Phone / fax / e-mail ______________________________

5. Represented by ______________________________

6. Sex	**7. Age**	**8. School degree**	**9. Time in**
___ Male	___ 16-30	___ High School	___ < 5 years
___ Female	___ 31-50	___ Technical	___ 5-10 yrs.
	___ 51-65	___ Undergraduate	___ 10-20 yrs.
	___ > 65	___ Graduate	___ > 20 yrs.

10. What is your institution role in land degradation management / assessment ?

____

11. What type(s) of cartography is used ? ______________________________

____

12. Is any model used ? No ___ Yes ___ Which one and what for ? ______________

____

13. Do you consider your institution able to incorporate new models ? No___Why ?

______________________ Yes___ Under what conditions ? ______________

14. Do you consider your institution interested in incorporating new models ?

No ___ Why ? ______________________________

Yes___ Under what conditions ? ______________________________

14. What are the main needs for cartography, satellite imagery and modelling ?

____

Date ___ / ___ / ______ *Place* ______________ *Done by* ______________
Observations ______________________________